AN ABSTRACT OF THE THESIS OF

David S. Princehouse for the degree of Master of Science in Geology presented on June 4, 1993

Title: Geology and Gold Mineralization of Mesozoic Rocks in the Pine Grove District, Lyon County, Nevada.

Abstract approved: Redacted for Privacy

John H. Dilles

The Pine Grove gold mining District is located in the Pine Grove Hills 34 km south of Yerington, west-central Nevada, in a large structural block consisting of Mesozoic granitoid rocks overlain by Cenozoic volcanic and sedimentary rocks. Hydrothermal alteration and associated gold mineralization is genetically and temporally linked with porphyry dikes that are cogenetic with the early Mesozoic host rock, the granodiorite of Lobdell Summit. Subsequent regional metamorphism altered the granitic rocks to low a greenschist facies, and ductile deformation imparted a weak foliation marked by metamorphic biotite. The Mesozoic rocks were tilted 20-25° W post Early Jurassic and prior to 15 Ma. Early Basin and Range faulting 15-7.5 Ma occurred along the Pine Grove Hills normal fault system bounding the east side of the hills. These faults tilted all rocks 30-40° W, and localized syn-tectonic clastic sediments of the Morgan Ranch Formation to the east. At the Wheeler Mine, two strands of this fault system strike N 60° W and

dip 25° E and have a total normal separation of 6-7 km. The eastern Wheeler Fault juxtaposes Morgan Ranch Formation against Mesozoic rocks. Lying 100 m to the west, the Stonehouse Fault has in excess of 500 m of offset. The Mesozoic rocks between the two faults are extensively faulted, cataclastically deformed, and contain gold ores, whereas Mesozoic rocks west of the Stonehouse Fault represent deeper, less mineralized parts of the hydrothermal system.

This study used detailed field mapping of surface and underground exposures and detailed logging of drill core and reverse circulation cuttings to determine the relationships and distribution of igneous, structural, alteration, and mineralization events at the Wheeler Mine. The petrologic studies, which include petrographic, electron microprobe, X-ray fluorescence, and instrumental neutron activation analyses, constrain the mineralogy and petrology of the host rocks and the subsequent hydrothermal alteration and mineralization.

The late Triassic or early Jurassic granodiorite of Lobdell Summit is the main host rock in the Pine Grove district. The granodiorite is intruded by six granitic dikes that strike north to northwest and dip 30-35° E, and are spatially and temporally related to mineralization. The similar major and trace element compositions of the granodiorite and granitic dikes indicate they genetically related and have similar ages. These granitic rocks are part

of a calc-alkaline, differentiated suite characterized by high potassium, a strong light rare earth element enrichment pattern, elevated Cs, Rb, U, and Th contents, and accessory allanite. Igneous hornblende geobarometry indicates the deposit formed at a depth of 7-10 km. This conclusion is supported by a minimum estimated 3-4 km depth made by construction of cross-sections.

The hydrothermal alteration in the Mesozoic granitic rocks can be classified from oldest to youngest based on cross-cutting field relations: the sequence is potassic, sodic, and sericitic. Potassic alteration is characterized by the replacement of hornblende by secondary biotite. The potassic alteration is limited to the granodiorite of Lobdell Summit and the three oldest granitic dikes. Sodic alteration is characterized by replacement of potassium feldspar by albite or oligoclase with or without the replacement of mafic minerals by actinolite and chlorite. Sericitic alteration is characterized by replacement of host rock by quartz-sericite-pyrite.

Gold and copper sulfide mineralization occur in transitional veins and vein selvages that are interpreted to be a transition from early potassic and sodic alteration to the late sericitic alteration. Gold and sulfide minerals are commonly absent from the potassic and sodic alteration, and gold is absent from sericitic alteration. The transitional vein assemblages consist of quartz-sulfide and chalcopyrite-pyrite veins having narrow selvages in which the rock is

partially converted to chlorite-sericite-albite. The sulfide minerals in these veins are pyrite, chalcopyrite, marcasite, and pyrrhotite, and these minerals also occur as disseminated grains around sulfide and quartz-sulfide veins. Native gold occurs in quartz-sulfide veins along the margins of pyrite and chalcopyrite grains or as inclusions in pyrite grains. There is a general positive correlation between gold and copper grades in the Wheeler Mine, but the gold/copper ratio increases upward in the mine over 200 m. The mineralization at the Wheeler Mine affected approximately 0.003 km^3 of rock and has grades of 0.03 to 3 ppm Au and 100 to 1000 ppm Cu.

The Pine Grove District is interpreted as a Au-rich Cu-poor porphyry copper-type deposit on the basis of the granite porphyry dikes, the associated potassic, sodic, and sericitic hydrothermal alteration types, and the localization of Au-Cu mineralization within quartz-pyrite-chalcopyrite veins.

Geology and Gold Mineralization of Mesozoic Rocks in the Pine Grove District, Lyon County, Nevada.

by

David S. Princehouse

A THESIS

Submitted to

Oregon State University

in partial fulfillment of

the requirements for the

degree of

Master of Science

Completed June 4, 1993

Commencement June, 1994

APPROVED:

Redacted for Privacy

Assistant Professor of Geology in charge of Major

Redacted for Privacy

Chairman of the Department of Geosciences

Redacted for Privacy

Dean of Graduate School

Date thesis is presented June 4, 1993

Thesis presented David S. Princehouse

ACKNOWLEDGEMENTS

I am greatly indebted to Dr. John Dilles for his advice, support, and friendship on this project. I would also like to thank the other members of my committee, Dr. Cyrus Field, Dr. Anita Grunder, and Dr. Martin Fisk, for their time and input.

I would like to thank to Teck Resources Inc. for their financial help and access to their exploration data on the Pine Grove District. Thanks to the OSU Radiation Center staff, especially Dr. Bob Walker, for the reactor time and facilities for INAA. Thanks also to the Department of Geosciences for the electron microprobe analyses.

Special thanks to Peter Wampler and John Doucette for their assistance with the computers.

I would like to thank the members of my family for their support, assistance, and understanding over the years. Special thanks to my mother, Anita Princehouse, for her patience, love, and motivation.

TABLE OF CONTENTS

List of Figures

List of Figures

LIST OF TABLES

List of Plates

Geology and Gold Mineralization of Mesozoic Rocks in the Pine Grove District, Lyon County, Nevada.

INTRODUCTION

The Pine Grove District is located in the Pine Grove Hills, in west-central Nevada. The District consists of two major properties, the Wilson and Wheeler Mines, and several smaller properties and prospects. The alteration and mineralization in the Wheeler Mine occurs in the Mesozoic granitic intrusions that compose the basement rocks of the Pine Grove Hills structural block. Recent exploration work by Teck Resources Inc. (1989-1992) in the Wheeler Mine and adjacent areas provided good access to the study area and a data base that included drill cuttings, drill core, and assays. This allowed the mineralization and alteration in the granitic rocks at the Wheeler Mine to be described and characterized in detail. The Wilson Mine lies to the northwest and has mineralization and alteration similar to the Wheeler Mine, but it is further from the Wheeler Fault so that deposit has not undergone the same deformation as the Wheeler Mine deposit. The Wilson Mine was not studied herein.

Location and Accessibility

The Pine Grove District is located in the Pine Grove Hills, 21 miles south of Yerington, Lyon County, Nevada (Figure 1). The district lies within Townships 9N and 10N and Ranges 25E and 26E, depicted on the Pine Grove Hills, Nevada, U.S.G.S. 15 minute quadrangle map.

Access to the district is by travelling 20 miles south of Yerington along State Highway 208 and then on the Pine Grove Flat road. From there, an unimproved road leads southwest 5 miles to the district.

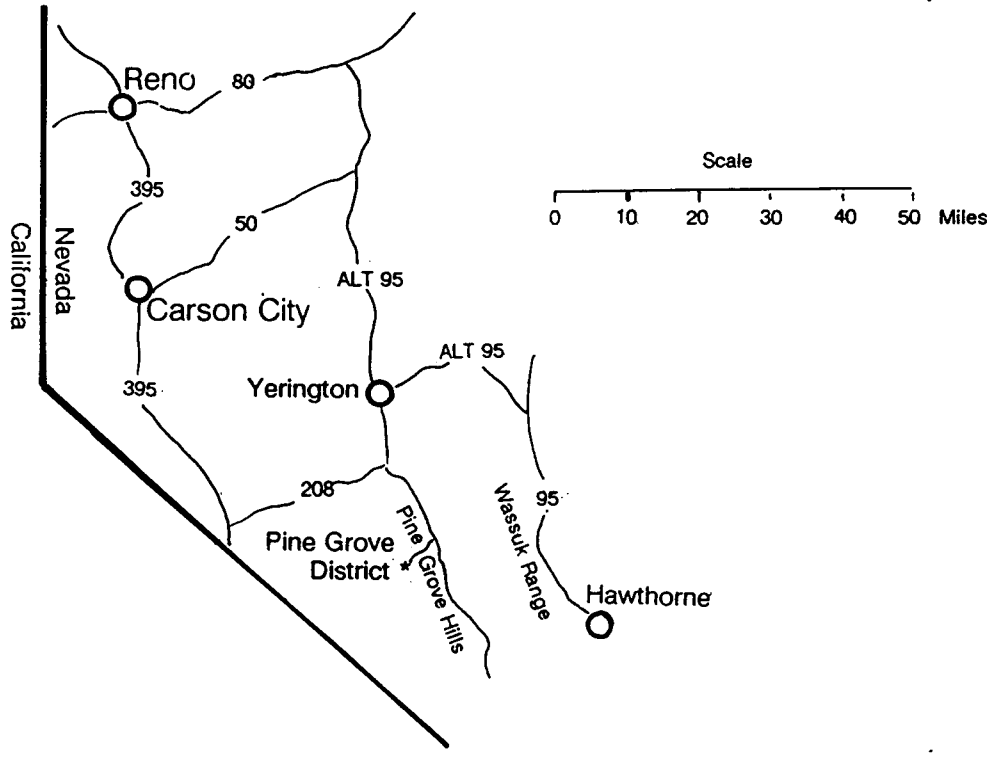

Figure 1. Location map for the Pine Grove District, Lyon County Nevada.

History and Production

The Pine Grove District was discovered by William Wilson in July, 1866. He located the Wilson Mine on the north side of Pine Grove Canyon, and a short time later the Wheeler Mine was located on the south side of the canyon. By 1882, the Wheeler Mine was operating a 15-stamp mill and the Wilson Mine a 10-stamp mill. Most of the district's gold and silver production was from these two operations between 1866 to 1871. The total production from the two operations has been estimated to be from $188,279 (Couch and Carpenter, 1943) to $5,000,000 (Lincoln, 1923) and $8,000,000 (Hill, 1915). In 1900, the Wilson Mine was acquired by Cutting and Hudgens, and the Wheeler Mine was bought by Pope and Talbot. These properties were worked by various lessees to present. The Wheeler Mine property was acquired in 1989 by Teck Resources Inc. They have done reconnaissance mapping, core drilling, reverse circulation drilling, and extensive surface and underground sampling of the Wheeler Mine area.

Previous Geologic Work

Some of the earliest published work on the Pine Grove District was done by J.M. Hill (1915). Hill described in detail the geology, alteration, and mineralization of the district in USGS Bulletin 594.

Brief descriptions of the district's history, production, and geology were included by F.C. Lincoln (1923) in "Mining Districts and Mineral Resources of Nevada", and by Stoddard and Carpenter (1950) in "Mineral Resources of Storey and Lyon Counties, Nevada", University of Nevada Bulletin 64.

The geology of Lyon, Douglas, and Ormsby Counties, Nevada was mapped on a scale of 1:250,000 by J.G. Moore (1969). This was published in the Nevada Bureau of Mines Bulletin 75, which includes a very brief description of the district by N.L. Archbold. Gilbert and Reynolds (1973) mapped the eastern margins of the Pine Grove Hills on a scale of 1:62,500, and Stewart and Reynolds (1987) mapped the geology of the Pine Grove Hills Quadrangle, Lyon County Nevada on a scale of 1:62,500.

The most comprehensive work done on the district was by P.E. Dircksen (1975). He described and compared the Pine Grove Mining District with the nearby Rockland Mining District in a master's thesis for the University of Nevada at Reno. Part of the work done by Dircksen included mapping the surface and underground exposures and doing some petrography on rock units.

Objectives

The main objectives of this investigation were to describe the geology of the Pine Grove gold deposit, develop a geologic model to explain its origin, and to compare this deposit to preexisting models, particularly those of porphyry copper origin. The specific objectives were to characterize original minerals and rock types, to characterize the alteration minerals and their assemblages, and to develop the chronology of igneous, structural, and alteration and mineralization events.

Method of Study

The following methods were used to achieve the objectives of this investigation:

1. Geologic mapping of surface exposures in the Wheeler Mine in a area of 610 m (2000 ft) by 915 m (3000 ft) on a scale of 1:600 and geologic mapping of over 685 m (2250 ft) of underground workings on a scale of 1:240. This work was done to determine the relationships and distribution of igneous, structural, alteration, and mineralization events.

2. Petrologic studies of the Wheeler Mine rocks to constrain the mineralogy and petrology of the hydrothermal mineralization and alteration, and the host rocks. These

studies included petrographic, electron microprobe, X-ray fluorescence, and instrumental neutron activation analyses.

Over two hundred and fifty samples were collected during field work. From representative samples, petrographic examination was done on 97 thin sections and 40 polished thin sections to identify primary igneous and secondary hydrothermal minerals, textural relations, paragenetic sequence of alteration and mineralization, and igneous rock types.

Electron microprobe analyses were done at Oregon State University using a Cameca SX-50. Over two hundred analyses were done on feldspars, micas, amphiboles, magnetite, ilmenite, titanite, and allanite to determine igneous and alteration mineral compositions. Operating conditions were a beam diameter of 20 microns, an accelerating potential of 15 keV, and counting times of 10 seconds for major and trace elements and 20 seconds for rare earth elements. Natural and synthetic minerals were used as standards and replicate analyses of standards were preformed. Precision on major and trace elements is estimated to better than 1% except for Fe and F ($\leq$ 3%). Precision on the REEs, Y, Th, and U is estimated to be between 1 and 4% or 0.02 wt.% oxide (detection limit), whichever is larger.

Chemical analyses were done on fifteen representative whole rock samples selected to characterize rock and alteration types. Samples for chemical analyses were crushed

in a jaw crusher with 99.5% pure alumina ceramic plates. A representative split of each crushed sample was powdered to less than 200 mesh in a SPEX alumina shatterbox for instrumental neutron activation analyses (INNA) or a SPEX tungsten carbide shatterbox for X-ray fluorescence (XRF).

Trace element analyses were done at the Oregon State University Radiation Center by INAA. Samples and standards were irradiated in a rotating rack in a TRIGA reactor for eight hours under a neutron flux of 3 X 10^{12} neutrons per cm^2 per second. Equivalent amounts of NIST standards SRM-1633a and OSU Radiation Center standards Allende and CRB-II were irradiated with the samples. Samples and standards were allowed to decay for seven days before each gamma ray spectrum was collected for 4000 seconds on a Ge-Li detector coupled with a 2048 channel pulse-height analyzer. After a additional seven days of decay, a gamma ray spectrum was collected for 4000 seconds on a LEP detector. When six to eight weeks of decay had occurred, a gamma ray spectrum was collected for 20,000 seconds on a Ge-Li detector coupled to the 2048 channel pulse-height analyzer. The uncertainties for Sc and La analyses are 3%, and the uncertainties for Co, As, Sb, Se, Cs, Sm, Eu, Tb, Yb, Lu, Hf, Ta, Au, Hg, and Th analyses 5%. The uncertainties for Ce and U analyses are 7%, the uncertainty for Cr analyses are 10%, and the uncertainties for Nd and W analyses are 12%.

Major element analyses were done by the Geology Department, Washington State University, Pullmam Washington by XRF using a Automatic Rigaku 3370 Spectrometer. The powdered rock samples (3.5 grams) were mixed with 7.0 grams of lithium tetraborate for ten minutes. The mixed powders were loaded into graphite crucibles and then placed in a preheated muffle furnace. The samples were heated for five minutes at a temperature of 1000°C. The crucibles were then removed and allowed to cool for ten minutes. Each glass disk was then reground in a Tema swingmill for 35 seconds. Then the powders was placed back in crucibles and reheated for five minutes at 1000°C. The glass disks were then ground with a coarse (240) SiC grit and a fine (600) SiC grit and then cleaned. The disks were then analyzed on the X-ray spectrometer which is in-line with a computer. The concentrations of 27 elements in the unknown samples were measured by comparing the X-ray intensity for each element with the intensity of two disks of eight international standards (USGS standards PCC-1, BCR-1, BIR-1, DNC-1, W-2, AGV-1, GSP-1, and G-2, using the values by Flanagan, 1976). Precision on major elements is estimated at better than 1% except for FeO, MnO, P_2O_5, MgO, and Na_2O ($\leq$ 3%). For trace elements, precision is estimated as better than 2 to 10%.

3. Geologic logging of over 186 m (610 ft) of core from two diamond drill holes and 1157 m (3795 ft) of cuttings from ten reverse circulation drill holes was done

to determine the relationships and distribution of igneous, structural, alteration, and mineralization events.

In brief, this investigation has produced detailed maps of rock type, structure, and zones of hydrothermal alteration. Estimates of chemical gain or loss associated with hydrothermal alteration have been calculated. Identification of mechanisms relating to gold-base metal sulfide mineralization and the corresponding metal zonation were established. These data were integrated into an improved geologic and geochemical model for the gold mineralization in the Wheeler Mine, which evaluates the role of porphyry type Au mineralization and provides a basis for the exploration of similar mineral deposits.

Regional Geology

The Pine Grove District is located in the Pine Grove Hills structural block described by Gilbert and Reynolds (1973). This structural block consists of Mesozoic plutons and Tertiary sedimentary and volcanic rocks. At least one period of Basin and Range deformation has uplifted these rocks.

The basement rocks of the Pine Grove Hills structural block are composed of two large Mesozoic plutons named and described by G. Nowark (1979): the porphyritic granite of Nye Canyon in the south and west, and the granodiorite of Lobdell Summit in the north (Figure 2). The Pine Grove District is hosted in the late Early Jurassic granodiorite of Lobdell Summit. A Jurassic age is indicated by Rb-Sr whole-rock isochrons ages of 186.9±8.5 Ma (John and others, in press) and 186.5±7.7 Ma (Robinson and Kistler, 1986).

The granodiorite is similar to other plutons of this age in the region (i.e., granite of Baldwin Canyon, which crops out in the southern Wassuk Range 5 km southeast of the southernmost exposure of the granodiorite of Lobdell Summit, and the granitic rocks of Babbit and Cottonwood Creek, which lie 30 km to southeast of the Pine Grove District on the north and south sides of Mount Grant in the central Wassuk Range). These plutons have a high ratio of igneous hornblende to igneous biotite (>1:1) and have undergone

Figure 2. Regional geology map of the Pine Grove Hills (Based on Stewart and Reynolds (1987) and author's own 1990 field mapping).

Tr - Rhyolite (late Miocene)
Tw - Morgan Ranch Formation (Miocene)
Tcv - Coal Valley Formation (Miocene)
Tb - Basalt (Miocene)
Ta - Andesitic and dacitic flows and breccias (Miocene)
Knc - Granite of Nye Canyon (Cretaceous)
Jgd - Granodiorite of Lobdell Summit (Jurassic)

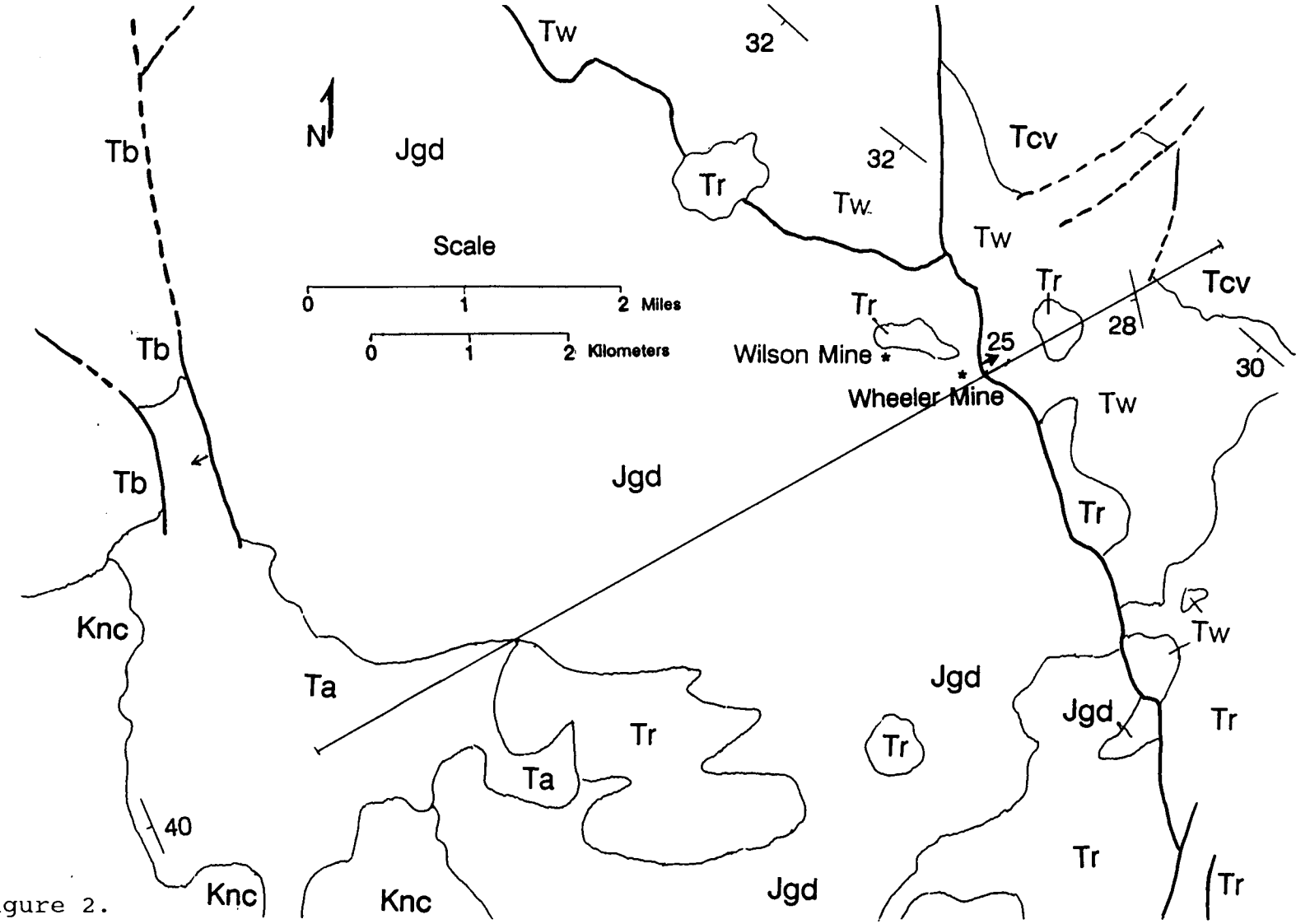
N
Scale
0 1 2 Miles
0 1 2 Kilometers
Tw
32
Jgd
Tr
32
Tcv
Tw
Tw
Tb
Tr
Tr
Tcv
Tb
Wilson Mine
25
28
30
Wheeler Mine
Tw
Tb
Jgd
Tr
Knc
Tw
Ta
Jgd
Tr
Jgd
Tr
Ta
Tr
40
Tr
Knc
Knc
Jgd
Tr
Tr

Figure 2.

metamorphism (John and others, in press). This metamorphic alteration is characterized by secondary biotite partially replacing hornblende grains. Dilles and Wright (1988) also described this metamorphic alteration for the 232.7±2.9 Ma Wassuk metadiorite and associated volcanic rocks in the northern Wassuk Range. The early quartz monzodiorite phase (169.4 Ma) of the Yerington Batholith (which lies 30 km to the north of Pine Grove District) crosscuts these Triassic age rocks so the age of deformation is constrained to post-233 Ma and pre-169.4 Ma (Dilles and Wright, 1988).

The nearby Middle Jurassic age (169-168 Ma) Yerington Batholith generally has hornblende to igneous biotite ratio ≥1:1 (Dilles, 1987). The Bear quartz monzonite and Luhr Hill porphyritic granite intrusions of the Yerington Batholith have coarse potassium feldspar megacrysts while the McLeod Hill quartz monzodiorite does not (Dilles, 1987).

In the Nye Canyon area (approximately 12-15 km to the south-southwest of the Pine Grove District), the Cretaceous granite of Nye Canyon has K-Ar ages (biotite) of 89.2±2.8 and 92.3±2.8 Ma (Krueger and Schilling, 1971; recalculated using 1976 IUGS constants, Steiger and Jager, 1977) and a four-point Rb-Sr whole-rock isochron age of 84.2±6.7 Ma (Robinson and Kistler, 1986). The granite of Nye Canyon is typical of other Cretaceous age plutons in the region in that it has a ratio of igneous hornblende to igneous biotite

less than one and has coarse potassium feldspar megacrysts (John and others, in press).

The granodiorite of Lobdell Summit in the Pine Grove District is intruded by at least six granitic intrusions, described below. These granitic dikes in the Pine Grove District are not dated, but some of these dikes do have the characteristics of the Jurassic plutons in the region. The Wheeler granite porphyry dike has a hornblende to igneous biotite ratio much greater than one and has numerous large potassium megacrysts. Also, the granodiorite of Lobdell Summit and the granitic rocks intruding it in the Pine Grove District all contain allanite in significant amounts. J.H. Dilles and D.A. John (personal commun., 1993) have found allanite in other plutons of late Triassic to early Jurassic age in the region (i.e., The Wassuk diorite, Strosnider Ranch pluton, granite of Thorne, West Walker pluton, Crow Spring pluton, and Frazier's Well pluton). This suggests that they all had a common source in a period of late Triassic to early Jurassic magmatism.

K-Ar radiometric dating from the district on hydrothermal biotite yields an age of 80.8±2.4 Ma (Gilbert and Reynolds, 1973; recalculated using 1976 IUGS constants, Steiger and Jager, 1977) and on hydrothermal muscovite yields an age of 85.9±2.0 Ma (Kleinhampl and Silberman, unpub. data; in John and others, in press). My interpretation is that these K-Ar dates probably represent

the age of the Cretaceous metamorphic resetting of older hydrothermal alteration. The ages given by hydrothermal micas are very similar to the age of the nearby Cretaceous granite of Nye Canyon, which could be responsible for resetting the K-Ar systems in the micas.

Andesitic and dacitic flows and breccias (unit Ta, Figure 2 and 3) lie in angular unconformity above the granitic basement in the region (Gilbert and Reynolds, 1973; Stewart and Reynolds, 1987). These Miocene rocks are widespread and are locally thick (approximately 500 m in the Cambridge Hills) in western Nevada and in the Sierra Nevada region north of Mono Lake, California (Gilbert and Reynolds, 1973). An andesite flow in the Cambridge Hills east of the Pine Grove District has a hornblende K-Ar age of 15.30±0.05 Ma (Gilbert and Reynolds, 1973; recalculated using 1976 IUGS constants, Steiger and Jager, 1977). In the Pine Grove Hills region these rocks crop out along the western edges of the Pine Grove and Cambridge Hills (Stewart and Reynolds, 1987).

The Miocene volcanic rocks are overlain by late Miocene sedimentary rocks that are part of the Wassuk Group, initially named and described by D.I. Axelrod (1953). The Wassuk Group is composed of the Aldrich Station, Coal Valley, and Morgan Ranch Formations (units Tcv and Tmr, Figure 2 and 3) with a total thickness of approximately 2,625 m near the Pine Grove District. The Aldrich Station and Coal Valley Formations are Miocene in age and are

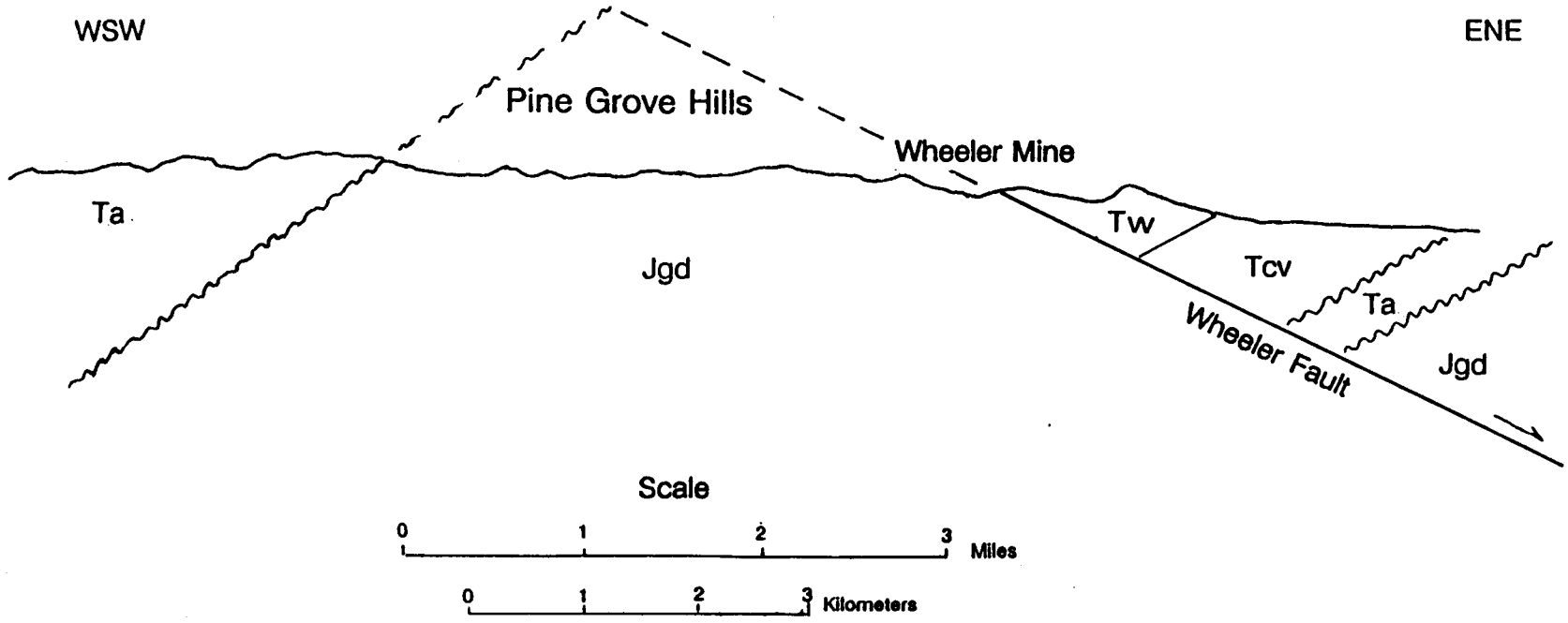

Figure 3. Regional cross section across the Pine Grove Hills based on Stewart and Reynolds (1987) and author's own 1990 field mapping. Cross section is oriented N 60° E and the Wheeler Mine is located in the footwall of the Wheeler Fault.

fluvio-lacustrine deposits composed of andesitic detritus with numerous tuff beds (Gilbert and Reynolds, 1973). The Aldrich Station Formation thins northward along the Wassuk Range and appears to be absent around the Pine Grove District.

The Morgan Ranch Formation is the youngest member of the Wassuk Group with an age of Late Miocene and possibly Pliocene, and is the only member to crop out in the Pine Grove District. The Morgan Ranch Formation mainly consists of coarse basement detritus from local structural blocks with a few tuff beds (Gilbert and Reynolds, 1973). Axelrod (1953) determined that the Morgan Ranch Formation near the Pine Grove District was approximately 1,225 m thick.

The Pine Grove Hills structural block is delineated by northwest striking faults of a early period of Basin and Range faulting (Gilbert and Reynolds, 1973). Structural blocks formed during this early period of deformation in the region typically have strikes of northwest or northeast to east. These early faults are younger than 15 Ma and older than 7.5 Ma. They have not been reactivated during later Quaternary deformation of the region. Younger faults in the region are characterized by having strikes of north or north-northwest.

The Pine Grove Hills fault zone belongs to this early period of Basin and Range faulting (Gilbert and Reynolds, 1973). This fault zone forms the northeast margin of the

Pine Grove Hills structural block, and it includes the Wheeler Fault. Figure 3 is a regional cross section across the Pine Grove Hills. The Wheeler Fault has had approximately 6-7 km of normal displacement on the basis of offset of the Miocene volcanic rocks (unit Ta). Along the Pine Grove Hills fault zone, the Wassuk Group units are confined to the downthrown block (Gilbert and Reynolds, 1973; Stewart and Reynolds, 1987). This displacement suggests that movement along the fault zone began in syn-Morgan Ranch time, resulting in the removal of the older strata and exposing the basement rocks west of the fault zone as the Morgan Ranch strata were accumulated.

The youngest rock in region is a Tertiary rhyolite. This rhyolite forms dikes and small plugs that intruded into the earlier rock units along pre-Quaternary Basin and Range faults such as the Wheeler Fault in the Wheeler Mine area. It occurs quite extensively in the central and eastern parts of the Pine Grove Hills and along the eastern margins of the range (Stewart and Reynolds, 1987). The rhyolite has biotite, sanidine, and plagioclase K-Ar ages that range from 5.7±0.1 Ma to 7.6±0.2 Ma (Gilbert and Reynolds, 1973; recalculated using 1976 IUGS constants, Steiger and Jager, 1977).

Large parts of the Wheeler Mine area are covered by a relatively thin layers of unconsolidated surficial deposits that obscure many bedrock exposures and contact

relationships. These deposits are Quaternary in age and are divided into two map units: alluvium (unit Qal, Plate 1 and 2) and tailings and road fill (unit Qdr, Plate 1 and 2). Alluvium includes recent stream sediments consisting of unconsolidated and nonsorted or poorly sorted sand, gravel, and boulders. Tailings and road fill is unconsolidated material from the excavation of the surface and underground mine workings and the construction the numerous drill roads.

GEOLOGY OF THE PINE GROVE DISTRICT

The Pine Grove District lies along the northeast margin of the granodiorite of the Lobdell Summit with the Wheeler Mine being located at the contact between the Mesozoic granitic rocks and Tertiary sedimentary rocks (Plate 1). All the major faults and intrusions in the district strike north-northwest and dip to the east.

Summary Chronology of Events

The chronology of events at the Pine Grove District is complex due to later events overprinting and obscuring earlier events. The emplacement of the Mesozoic granitic rocks and the hydrothermal alteration that affected them probably took place within a relatively short period of time based on field relations and a comparison of this deposit to other similar deposits (Dilles and Einaudi, 1992). Unfortunately, there are no age dates to confirm if this is the case: the K-Ar dates mentioned above probably were reset by later thermal events. More data to support the summary here are included in following sections.

The first event was the emplacement of the granodiorite of Lobdell Summit. The granodiorite has a whole-rock Rb-Sr age of 186.9±8.5 Ma (John and others, in press) and 186.5±7.7 Ma (Robinson and Kistler, 1986). The granodiorite

may be older because a metamorphic event described later herein has effected granodiorite and possibly reset the Rb-Sr isochron. The granodiorite was then intruded by first, the Wheeler granite porphyry and then, the microdiorite dikes. The monzonite dike(s) were emplaced sometime during this sequence, but there is no indication of when this took place.

The next major event was potassic alteration characterized by biotite (described in greater detail later within). This alteration replaced igneous mafic minerals in the Mesozoic rocks with biotite.

Next, the quartz porphyry and then the hornblende granite porphyry dikes were emplaced into the granodiorite of Lobdell Summit and Wheeler granite porphyry. These two dikes were not potassically altered as the previous Mesozoic rocks were.

After the emplacement of the porphyry dikes, sodic alteration occurred in the Pine Grove District. This alteration affected all of the Mesozoic granitic rocks, especially the quartz porphyry and hornblende granite porphyry dikes. It was during this event when actinolite and epidote veins were formed.

Quartz-sulfide and sulfide veins that are a transition from potassic alteration to sericitic alteration occurred next (described later within). These veins contain the gold and copper mineralization that occurs in the Wheeler Mine.

The next and last hydrothermal event was the sericitic alteration which affected all of the Mesozoic granitic rocks in the Pine Grove District.

The age of the aplite dikes in the district is unclear. Aplite dikes are altered between the Wheeler and Stonehouse Faults, but to the west of the Stonehouse Fault the dikes are not altered. It is possible that there were two periods of aplite dike emplacement, or that the dikes were emplaced during and after hydrothermal alteration.

A regional metamorphism to low greenschist grade altered the Mesozoic granitic rocks after hydrothermal alteration took place in the Pine Grove District. Dilles and Wright (1988) constrained the age of this metamorphic event in the nearby Yerington area to between 169 Ma and the earliest Jurassic, post-dating 233-232 Ma plutons. The granitic dikes in the mine area were tilted 20-25° west, possibly during this metamorphic event or a subsequent tectonic event.

The next event to take place region was the emplacement of Cretaceous plutons near the Pine Grove District. The Cretaceous granite of Nye Canyon has a K-Ar ages of 89.2±2.8 and 92.3±2.8 Ma (Krueger and Schilling, 1971; recalculated using 1976 IUGS constants, Steiger and Jager, 1977) and a four-point Rb-Sr whole-rock isochron age of 84.2±2.8 Ma (Robinson and Kistler, 1986). The Cretaceous plutons reset

the K-Ar ages in the district to the age of the granite of Nye Canyon.

After the regional metamorphic event and the emplacement of the Cretaceous plutons, the Mesozoic granitic rocks were eroded until andesitic and dacitic flows and breccias were emplaced at about 15 Ma.

There was then a period of deformation which tilted the area about 5-10° to the west (Stewart and Reynolds, 1987). This deformation took place between emplacement of andesitic and dacitic volcanic rocks and the early Basin and Range fault deformation,the latter which is constrained between 15-7.5 Ma (Gilbert and Reynolds, 1973). In the Wheeler Mine area, this deformation formed the Wheeler and Stonehouse Faults, which separate the Mesozoic granitic rocks in the west from the Tertiary sedimentary rocks in the east. The Basin and Range deformation has tilted the rocks about 30° to the west. The Morgan Ranch Formation formed in the late Miocene during this period of early Basin and Range deformation.

The last major geological event in the Pine Grove District was the emplacement of Tertiary rhyolite intrusions between 7.6±0.2 and 5.7±0.1 Ma (Gilbert and Reynolds, 1973). Since then man and stream processes have formed thin Quaternary units in the district.

Emplacement of the Mesozoic Igneous Rocks

At the Wheeler Mine, the Granodiorite of Lobdell Summit (unit Jgd, Plate 1) is intruded by at least six successive, Mesozoic granitic intrusions that crop out on the surface and/or are intersected by underground workings and exploration drilling. The oldest and largest of these granitic intrusions is the Wheeler granite porphyry (unit Jgp, Plate 1). The granite porphyry dike crops out west of the Wheeler Mine and is intersected by some of the deeper exploration drill holes. This dike is up to 18 m wide, strikes north-northwest, and dips approximately 40° to the east.

The granodiorite of Lobdell Summit and the Wheeler granite porphyry are intruded by numerous microdiorite dikes (unit Jmd, Plate 1). These dikes are generally 1-2 m wide, but some are as wide as to 5 m in the underground workings at the Wheeler Mine. The dikes have no consistent strike or dip. Microdiorite dikes are found intruding the Wheeler granite porphyry dike and the granodiorite of Lobdell Summit east of this porphyry dike. The microdiorite dikes are probably present west of the Wheeler granite porphyry dike, but are not apparent due to poor exposure.

The third Mesozoic granitic intrusive event is emplacement of monzonite dike(s). The monzonite only intrudes the granodiorite of Lobdell Summit between the

Wheeler Fault and the Stonehouse Fault described below. It does not crop out on the surface in the Wheeler Mine area and is only exposed in 15 m (50 ft) of underground workings and five reverse circulation drill holes. The monzonite dikes are inferred to dip 70-80° to the east (Plate 2). The age of the monzonite is unknown compared to the Wheeler granite porphyry and microdiorite dikes, but it is inferred to be older than the quartz porphyry dikes because the monzonite has undergone potassium alteration and the quartz porphyry has not.

The fourth granitic intrusive event was the emplacement of the quartz porphyry dikes (unit Jqp, Plate 1). Quartz porphyry intrusions intrude the granodiorite of Lobdell Summit and the Wheeler granite porphyry dike. Although the quartz porphyry intrusions are not exposed intruding the microdiorite dikes, the quartz porphyry intrusions are inferred to be younger because the granodiorite of Lobdell Summit, Wheeler granite porphyry, microdiorite, and monzonite dikes have undergone potassic alteration and the quartz porphyry intrusions have not. The quartz porphyry intrusions form dikes and plugs that generally crop out west of the Wheeler granite porphyry and dip to the east below it. The largest of these quartz porphyry intrusions strikes north-northwest and dips approximately 30° to the east.

The last two Mesozoic intrusions are volumetrically smaller than previous intrusions. The hornblende granite

porphyry dikes (unit Jhp, Plate 1) were the fifth granitic intrusion to intrude the granodiorite of Lobdell Summit at the Wheeler Mine. The hornblende granite porphyry intrudes the granodiorite of Lobdell Summit, Wheeler granite porphyry, and quartz porphyry intrusions. Hornblende granite porphyry dikes are up to 5-7 m wide, strike north or northwest, and dip approximately 34° to east. Hornblende granite porphyry dikes are the last Mesozoic intrusions to have undergone pervasive hydrothermal alteration in the Wheeler Mine area. The youngest Mesozoic intrusive rocks in the area are the aplite dikes (unit Ja, Plate 1). The aplite dikes are found in the granodiorite of Lobdell Summit and the Wheeler granite porphyry. The dikes are not over 1-2 m wide, and are generally much less. The aplite dikes strike approximately north or northwest.

Structure at the Wheeler Mine

There are three ages of structures present in the Wheeler Mine area: Mesozoic granitic dikes, metamorphic foliation and ductile deformation, and Tertiary brittle deformation.

The oldest of these structures are the Mesozoic granitic dikes which are related to hydrothermal alteration and mineralization. These north-northwest striking dikes

were originally oriented vertically and have been tilted westward so that they dip 30-40° E.

The next set of structures in the Wheeler Mine area is related to the Jurassic metamorphic event that is younger than the hydrothermal alteration and mineralization. Dilles and Wright (1988) constrained the age of this metamorphic event to between 169 Ma and the earliest Jurassic, post-dating 233 and 232 Ma plutons. This metamorphic event aligned igneous and hydrothermal biotite grains in the granodiorite of Lobdell Summit to form a weak foliation. The foliation has a present orientation of north to northwest. This foliation cuts hydrothermal veins of biotite and quartz, and occurs both east and west of Stonehouse Fault away from the area of Tertiary faulting. The quartz in the granodiorite is commonly polygonalized, and quartz grains in folded quartz veins have triple junctions.

The youngest set of structures in the Wheeler Mine area is related to brittle, cataclastic deformation that is characterized by faults. These faults are part of a early period of Basin and Range faulting that occurred in the region between 15-7.5 Ma.

Major faults in the Wheeler Mine area have the same north-northwest strikes and easterly dips as the larger Mesozoic intrusions (i.e. Wheeler granite porphyry and quartz porphyry). The largest is Wheeler Fault, which separates the Mesozoic granitic rocks in the west from the

Tertiary Morgan Ranch Formation in the east (Plate 1). The Wheeler Fault strikes north-northwest, dips 22-25° to the east, and has 6-7 km of normal displacement, based on the cross sections A-A' and B-B' (Plate 2) and Figure 3. A small, poorly defined syncline, the axis of which parallels the Wheeler Fault, was formed in the Morgan Ranch Formation in the hanging wall of the fault due to drag.

Other major faults are not so apparent on the surface, but are exposed in the underground workings and from exploration drilling (Plates 2 and 6). A second major fault is the Stonehouse Fault that separates the mineralized rocks in the Wheeler Mine from the non-mineralized rocks to the west and is parallel to, and is 100 m (325 ft) below the Wheeler Fault (Plate 2). This normal fault strikes north-northwest and dips 25-28° to the east. The Stonehouse Fault has placed rocks from higher in the hydrothermal system on the east next to rocks lower in the system on the west and has an estimated offset of more than 100 m. There are several other large faults between the Wheeler and Stonehouse Faults, thus forming a major fault zone 90 m (300 ft) thick (Plate 2). They strike north-northwest also, but they dip 30-50° to the east.

The rock between the Wheeler and Stonehouse Faults has undergone extensive brittle deformation. The granodiorite of Lobdell Summit here has numerous small faults which generally strike N30°W to N60°W and dip to the northeast,

but many small faults strike and dip in seemingly random directions. There are a few small, north to northeast striking faults that offset the earlier north-northwest striking faults.

The granodiorite of the Lobdell Summit between the Wheeler and Stonehouse Faults commonly has been deformed to the extent that it has a cataclastic texture. Plagioclase grains are often broken or bent with twinning that is distorted. Biotite forms a foliation that is parallel to the Wheeler Fault and may be in part earlier Mesozoic ductile deformation and later, re-orientated Cenozoic brittle deformation (Plate 1). This brittle deformation decreases westward with distance from the Wheeler Fault. West of the Stonehouse Fault, deformation is less intense; here, in the Wheeler granite porphyry and quartz porphyry, the cataclastic deformation is characterized by broken and offset feldspar phenocrysts.

Igneous Petrography

Granodiorite of Lobdell Summit

The granodiorite of Lobdell Summit (unit Jgd, Plate 1) is equigranular, medium-grained, light to dark depending on the degree of alteration, and generally homogeneous except for inclusions of fine-grained, mafic-rich, irregular blebs up to 7 cm in diameter. All samples of the granodiorite in the Wheeler Mine area have undergone some degree of hydrothermal or metamorphic alteration.

The essential minerals of the granodiorite are plagioclase, microcline, quartz, hornblende, and biotite (Table 1). Minor and trace amounts of titanite, allanite, epidote, apatite, zircon, and opaque minerals are also present. Plagioclase is subhedral to euhedral, prismatic and lath-shaped, and is commonly 2-5 mm in length. Plagioclase has normal but oscillatory zonation, and ranges from An_{41} at the core to An_{13} at the rim (determined by electron microprobe). Microcline and quartz are interstitial with respect to plagioclase. Anhedral microcline has tartan twinning, is up to 1.75 mm in diameter, and is locally perthitic. Anhedral quartz does not have undulose extinction and is generally not more than 0.75 mm in diameter.

Hydrothermal or metamorphic alteration and deformation has resulted in the partial replacement of igneous

Table 1. Modal Mineralogy of the Pine Grove District Granitic Rocks in Volume Percent

Rock Type	Jgd	Jgp	Jmd	Jm	Jqp	Jhp	Ja
Sample	DSP	DSP	DSP	DSP	DSP	DSP	DSP
Number	225	237	3	41	190	165	230
Mineral:							
Plagioclase	41.5	24.2	67.5	31.0	7.0	19.6	17.2
Alkali Feldspar	11.8	$(4.7)_1$	----	$(55.3)_1$	$(3.0)_1$	----	38.4
Quartz	19.2	----	----	4.5	4.4	----	37.2
Groundmass	----	43.8	----	----	77.2	65.4	----
Alkali Feldspar		$(21.9)_1$			$(38.6)_2$	$(45.6)_2$	
Quartz		21.9			38.6	19.8	
Mafic minerals		Tr			Tr	Tr	
Hornblende	2.8	----	----	----	----	$(8.8)_3$	----
Estimated Original Igneous Hornblende	$(7.6)_4$	$(9.8)_4$	----	----	----	----	----
Igneous Biotite	5.8	2.0	----	----	6.8	0.6	7.0
Secondary Biotite	14.4	15.7	27.0	4.0	Tr	----	----
Chlorite	1.4	4.3	Tr	1.3	Tr	1.2	Tr
Sericite	Tr	Tr	----	3.8	----	----	----
Epidote	2.1	2.7	----	----	----	----	Tr
Titanite	Tr	1.6	----	Tr	----	----	----
allanite	Tr	Tr	Tr	----	Tr	Tr	Tr
Zircon	Tr	----	----	----	Tr	----	----
Apatite	Tr	Tr	----	Tr	Tr	1.0	----
Igneous Magnetite	1.0	1.0	----	----	Tr	4.0	----
Secondary Magnetite	----	----	5.5	----	----	3.0	----
Ilmenite	Tr	Tr	----	----	----	----	----
Rutile	Tr	Tr	----	----	Tr	----	Tr
Pyrite	----	Tr	----	----	----	----	----
Points	540	463	400	525	525	500	500

1. Estimated original content. Consists now of igneous K-Feldspar + secondary albite
2. Estimated original content. Consists now of secondary albite
3. Estimated original content. Consists now of secondary actinolite
4. Estimated original content. Consists now of igneous hornblende + (secondary biotite + chlorite + epidote + titanite in hornblende sites)

Tr = trace amounts

hornblende and has aligned biotite into a weak foliation. Euhedral igneous hornblende has light brown to green pleochroism and is as long 5 mm (Table 2 for electron microprobe analyses). Hornblende grains are commonly surrounded with reaction rims of secondary biotite, and in many cases, the igneous hornblende is completely replaced by secondary biotite (or chlorite), epidote, and titanite. Igneous biotite is subhedral to euhedral, up to 2 mm in length, and has yellowish brown to green pleochroism (Appendix 5). Igneous biotite is commonly rimmed by rutile, and has rutile needles in cleavages which are orientated in a hexagonal pattern producing a sagenitic texture. The rutile needles of exsolution origin formed from the titaniferous igneous mica and precipitated within the crystal structure under the influence of hydrothermal fluids (Lanier and others, 1978). Rutile needles maybe up to 0.02 mm in diameter and 0.12 mm in length.

Apatite, allanite, zircon, magnetite, and ilmenite only occur in trace amounts. Apatite forms euhedral rods up to 0.13 mm in length that are typically found in plagioclase grains. Anhedral allanite is up to 1.75 mm in diameter and has strong red to reddish brown pleochroism. Allanite in the granodiorite tends to have a higher cerium content in its core than in its rims (Appendix 2). Allanite occurs interstitially with respect to plagioclase grains. Zircon is very rare and occurs as euhedral grains up to 0.2 mm in

diameter. Igneous magnetite (X_{usp}=0.001, Appendix 3) is euhedral, up to 0.25 mm in diameter, and often occurs in mafic mineral clusters. Igneous ilmenite (X_{ilm}=0.969; Appendix 3) is subhedral to euhedral, up to 0.15 mm in diameter, and has titanite halos up to 0.04 mm wide. Ilmenite grains also have apatite grains as inclusions or along margins.

The secondary biotite has brownish green to green pleochroism, is generally not over 0.15 mm in length, and has a shreddy texture (Appendix 5). Shreddy texture is defined as randomly oriented aggregates of fine-grained, subhedral flakes. Only about 30% of the secondary biotite occurs in hornblende sites, the rest occurs along grain boundaries (50%) and in plagioclase (20%). Chlorite has pale green pleochroism with dark green to blue-green birefringence. Chlorite has replaced up to 10% of the secondary biotite in the least altered samples of granodiorite. This replacement chlorite still retains the shreddy texture of secondary biotite. Sericite is anhedral, up to 0.05 mm in length, and occurs as scattered grains lightly dusting plagioclase grains. Secondary epidote occurs as scattered, anhedral grains up to 1.25 mm in diameter in plagioclase grains or with secondary biotite replacing hornblende grains. Epidote also occurs as 1-10 mm wide veins that occasionally has selvages in which mafic minerals are destroyed. Titanite occurs as subhedral grains up to 0.5 mm

in diameter that replace hornblende grains together with secondary biotite and epidote, or as rims up 0.04 mm wide on ilmenite grains. Titanite in the granodiorite has a very small amount of rare earth elements (REEs) compared to titanite in the Wheeler granite porphyry (Appendix 1).

Based on texture and mineralogy, the protolith was a biotite-hornblende granodiorite using the IUGS classification system (Streckeisen, 1976). The original mafic mineral content was estimated to be 7-8% hornblende, based on relict igneous hornblende grains plus alteration biotite, chlorite, epidote, and titanite, and 5-6% igneous biotite based on relict igneous grains.

Wheeler Granite Porphyry

The Wheeler granite porphyry is pink to light grey with large pink, white, and green phenocrysts (unit Jgp, Plate 1). This porphyry has been altered, and occasionally displays a weak foliation marked by biotite. Phenocrysts of plagioclase, orthoclase, biotite, titanite, allanite, and opaque minerals make up 55-60 volume percent of the granite porphyry (Table 1). The rest of the porphyry consists of a groundmass (40-45 volume percent) consisting of quartz, alkali feldspar, and trace amounts of biotite. The groundmass is 0.02-0.06 mm in grain size and has a granophyric texture.

Subhedral plagioclase is albite (An_2 to An_9 composition determined by electron microprobe), is prismatic and lath shaped, and is up to 5 mm in length. Plagioclase phenocrysts are commonly dusted with sericite, biotite, and epidote, are embayed, and have a myrmekitic texture on the margins. Orthoclase phenocrysts are subhedral to euhedral and are up to 8 mm in length. The interiors of some orthoclase phenocrysts contain numerous euhedral plagioclase inclusions that are 0.12-0.35 mm in length and make up 60-65 volume percent of the phenocrysts. Orthoclase is optically continuous between the plagioclase inclusions and forms a 0.4-0.8 mm wide inclusion free rim. Hydrothermal albite partially replaces orthoclase phenocrysts, typically along the rims of phenocrysts. This hydrothermal albite has the characteristic short, irregular twins as described elsewhere (Gilluly, 1933; Carten, 1986).

Subhedral igneous biotite has light brown to green pleochroism, is up to 3 mm in length, and has some rutile in cleavages (Appendix 5). Secondary biotite has brownish green to green pleochroism, a shreddy texture, and is generally not over 0.12 mm in length (Appendix 5). Only a trace amount of secondary biotite replaces plagioclase phenocrysts, whereas 35% of the secondary biotite is in aggregates replacing hornblende phenocrysts and 65% of the secondary biotite occurs as scattered grains in the groundmass. Chlorite has pale green pleochroism with dark green to blue-

green birefringence and retains the shreddy texture of the replaced secondary biotite. Sericite is anhedral, up to 0.05 mm in length, and replaces plagioclase phenocrysts.

Titanite, epidote, apatite, allanite, and opaque minerals occur in minor and trace amounts. Igneous titanite forms subhedral rhombohedrons that are up to 0.9 mm in length. Igneous titanite in the granite porphyry has varying amounts of oxides of cerium (0.01 to 0.94 wt%), neodymium (0.0 to 0.58 wt%), samarium (0.01 to 0.14 wt%), and gadolinium (0.02 to 0.24 wt%), dysprosium (0.01 to 0.12 wt%), and ytterbium (0.0 to 0.1 wt%) (Appendix I). Titanite also occurs with epidote and secondary biotite in replacing hornblende phenocrysts. The secondary titanite is anhedral, up to 0.05 mm in diameter, and occurs in secondary biotite aggregates. Secondary epidote is anhedral, up to 1.25 mm in diameter, and occurs in secondary biotite aggregates and plagioclase phenocrysts. Anhedral allanite has strong red to reddish brown pleochroism, is up to 0.4 mm in diameter, and occurs interstitially. Apatite occurs as euhedral rods up to 0.1 mm in length in plagioclase phenocrysts. Subhedral igneous magnetite is up to 0.5 mm in diameter, and cubic pyrite is up to 0.1 mm on a side. Commonly magnetite and pyrite are partially rimmed by hematite.

This intrusion is classified as a biotite-bearing hornblende granite porphyry using the IUGS classification system (Streckeisen, 1976). The basis for this is that the

groundmass is estimated to contain equal amounts of alkali feldspar and quartz, and that all igneous hornblende has been replaced by secondary biotite, epidote, and titanite. Considering the alteration mineral aggregates, there may have been originally 9-10 volume percent igneous hornblende.

Microdiorite Dikes

The microdiorite dikes are light grey in color and are generally strongly magnetic (unit Jmd, Plate 1). This unit also is hydrothermally altered. The microdiorite is composed largely of anhedral to euhedral plagioclase grains from 0.1-0.7 mm in length (Table 1). The larger grains are more euhedral and are occasionally lightly dusted with secondary biotite. Hydrothermal magnetite and biotite occur interstitially between the plagioclase laths. Magnetite forms equant octahedra generally not more than 0.02 mm in diameter, but rare grains are up to 0.05 mm in diameter. Secondary biotite has brownish green to green pleochroism, a shreddy texture, and is not over 0.15 mm in length. A trace amount of secondary biotite has been replaced by chlorite. The chlorite retains the shreddy texture of the secondary biotite and has pale green pleochroism with dark green to blue-green birefringence.

Based on mineralogy and texture, the original protolith was a diorite that originally had 15-25% igneous mafic

minerals. Secondary biotite and magnetite have completely replaced the pyroxene, or possibly amphibole, originally present.

Monzonite

Monzonite is hydrothermally altered and has undergone much deformation (unit Jm, Plate 2). It is equigranular, medium-grained, and white to light green in color. The monzonite is largely composed of secondary albite, plagioclase, microcline, and secondary biotite, with minor amounts of quartz, chlorite, sericite, apatite, titanite, epidote, and calcite as described later (Table 1).

Anhedral microcline is tartan twinned and is up to 3.5 mm in diameter. Plagioclase is anhedral to subhedral, up to 1.5 mm in length, and commonly has broken and distorted twins. The plagioclase grains are often dusted with fine-grained sericite. Anhedral quartz is up to 1.0 mm in diameter (generally much less) and occurs interstitially with respect to microcline and plagioclase.

Titanite and apatite occur only in trace amounts. Igneous titanite forms subhedral rhombohedrons that are up to 0.2 mm in length. Apatite forms euhedral rods that are up to 0.1 mm in length and are commonly found in plagioclase grains.

The secondary minerals occur in minor and trace amounts. Over two thirds of the microcline has been partially or totally replaced by hydrothermal albite. This secondary albite has the characteristic short, irregular twins as described elsewhere (Gilluly, 1933; Carten, 1986). Secondary biotite has brownish green to green pleochroism, is up to 0.14 mm in length, and has a shreddy texture. The secondary biotite occurs along grain boundaries. Chlorite has pale green pleochroism with dark green to blue-green birefringence. Chlorite replaces about 15% of the secondary biotite, and this replacement chlorite still retains the shreddy texture of the secondary biotite. Sericite is anhedral and is generally not more than 0.05 mm in length, but sericite in veinlets can be up to 0.5 mm in length. Most sericite occurs in plagioclase grains where it dusts the grains. About 35-40% of secondary biotite has been partially or totally replaced by sericite. This sericite retains the shreddy texture of the secondary biotite and is coarser grained than most sericite present. There are also rare sericite veinlets that are up to 0.1 mm wide. Calcite occurs as scattered grains up to 0.15 mm in diameter in microcline grains, or as rare 0.15 mm wide veinlets.

Based on mineralogy and texture, the protolith was a monzonite using IUGS classification system (Streckeisen, 1976). The original igneous alkali feldspar content is estimated to have been 45-46%.

Quartz Porphyry

The quartz porphyry is white to pink in appearance and has characteristic distinct large quartz phenocrysts (unit Jqp, Plate 1). This porphyry also has been altered and deformed to some degree: there is no foliation present, but quartz phenocrysts commonly have undulose extinction and feldspar phenocrysts are broken and offset. Over 75 volume percent of the quartz porphyry is composed of 0.02-0.05 mm groundmass with a granophyric texture. The groundmass is estimated to have been originally about equal amounts of quartz and alkali feldspar (Table 1). Secondary albite has totally replaced the alkali feldspar in the groundmass. This secondary albite has the characteristic short, irregular twins of hydrothermal albite as described elsewhere (Gilluly, 1933; Carten, 1986). The other 25 volume percent is composed of phenocrysts of albite, quartz, biotite, apatite, zircon, chlorite, and pyrite, as follows. Euhedral plagioclase ranges from $An_{0.5}$ to $An_{1.4}$ (determined by electron microprobe), is up to 2.25 mm in length, and has a myrmekitic texture with quartz on the margins. Quartz is clear to grey, rounded, and ranges from 0.5 to 3 mm in diameter. Igneous biotite has brownish green to green pleochroism, is up to 0.3 mm in length, and has rutile in the cleavages (Appendix 5). Secondary albite has totally replaced euhedral alkali feldspar that was up to 3.75 mm in

length. This albite has the characteristic short, irregular twins of hydrothermal albite as described elsewhere (Gilluly, 1933; Carten, 1986). The secondary albite has rare inclusions of euhedral plagioclase up to 0.75 mm in length and very rare inclusions of anhedral quartz up to 0.05 mm in diameter also suggesting it replaced magmatic potassium feldspar crystals. Secondary biotite occurs as rare scattered grains or veinlets in the groundmass. Trace amounts of secondary biotite have been replaced by chlorite that retains the shreddy texture of the biotite. The chlorite has pale green pleochroism with dark green to blue-green birefringence. Cubic pyrite is up to 0.5 mm in diameter and is often partly or totally altered to hematite. Apatite occurs as euhedral rods up to 0.2 mm in length in plagioclase phenocrysts. Euhedral zircon is very rare and is up to 0.15 mm in diameter.

This rock is classified as a granite porphyry on the basis of the IUGS classification system (Streckeisen, 1976).

Hornblende Granite Porphyry

The hornblende granite porphyry dikes are grey in color, fine-grained, and contain numerous green actinolite phenocrysts (unit Jhp, Plate 1). These dikes have also been hydrothermally altered. The groundmass makes up 67 volume percent of the porphyry dikes with the rest of the volume

consisting of phenocrysts of plagioclase, amphibole, biotite, chlorite, allanite, and opaque minerals (Table 1). The equigranular groundmass is from 0.02-0.05 mm in diameter and is composed of irregular quartz (33 volume percent) and albite (66 volume percent) and euhedral apatite (1 volume percent). This groundmass albite has the characteristic short, irregular twins of hydrothermal albite as described elsewhere (Gilluly, 1933; Carten, 1986). Apatite occurs as rods that are 0.01 to 0.05 mm in length.

Euhedral plagioclase phenocrysts are up to 2 mm in length and range from An_1 to $An_{1.6}$ (determined by electron microprobe). These albite compositions are the result of hydrothermal alteration. Plagioclase has a myrmekitic texture at its margins. Amphibole phenocrysts are subhedral to euhedral, up to 1.25 mm in length, and have clear to light green pleochroism (Table 2). The amphibole originally was hornblende and has been altered to actinolite. Igneous biotite is subhedral, up to 0.5 mm in length, and has brownish green to green pleochroism. Chlorite retains the shape of the biotite it replaces. Chlorite has pale green pleochroism and dark green to blue-green birefringence. Allanite is anhedral and has strong red to brownish-red pleochroism. Igneous magnetite forms equant octahedra up to 0.3 mm in diameter. Hydrothermal magnetite is anhedral and is up to 0.1 mm in diameter, but is generally much less. Secondary magnetite is associated with actinolite

phenocrysts where it found on the margins or inside of the phenocrysts. Hematite occurs as rims on some magnetite phenocrysts.

Based on mineralogy and texture, the original protolith was a biotite-magnetite bearing hornblende granite porphyry using IUGS classification system (Streckeisen, 1976). There originally may have been 1-2 volume percent biotite and 46-47 volume percent alkali feldspar. The groundmass albite is thought to have replaced alkali feldspar because it has the short, irregular twinning common to hydrothermal albite.

Aplite Dikes

Aplite dikes are medium-grained, pink to white, and have a micrographic texture (unit Ja, Plate 1). Essential minerals are plagioclase, microcline, quartz, biotite, and epidote (Table 1). Minor and trace amounts of sericite, chlorite, titanite, allanite, and opaque minerals occur. Plagioclase is euhedral, up to 1.5 mm in length, and is commonly partly replaced by epidote and sericite. Anhedral microcline and quartz form the micrographic texture present in the dike. Microcline is up to 1 mm in diameter, and quartz is up to 0.4 mm in diameter. Igneous biotite is subhedral, up to 0.2 mm in length, and has light brown to green pleochroism. Chlorite replaces trace amounts of biotite. Chlorite has pale green pleochroism and dark green

to blue-green birefringence. Igneous titanite is subhedral and up to 0.4 mm in length. Anhedral allanite is up to 0.45 mm in diameter and has strong red to brownish red pleochroism. Anhedral epidote is up to 0.2 mm in diameter. Epidote also forms veinlets that are up to 0.25 mm wide and contain trace amounts of hematite. This hematite is up to 0.04 mm on a side and has replaced cubic pyrite. Anhedral sericite is up to 0.03 mm in length. About 50% of the plagioclase grains is lightly dusted with sericite.

Based on mineralogy and texture, the dikes are classified as biotite granites.

Tertiary Rhyolite

Tertiary rhyolite is pale pink to white, flow-banded, and occasionally has a 0.3 - 1.3 m wide, black vitrophyre exposed at the margins (unit Tr, Plate 1). The rhyolite is about 99 volume percent glass with the rest consisting of phenocrysts of sanidine, biotite, quartz, and plagioclase. Sanidine phenocrysts make up about 1 volume percent of the rhyolite, whereas the other minerals occur in only trace amounts. Sanidine phenocrysts are subhedral to euhedral, Carlsbad twinned, and are from 0.25-1.0 mm in length. Subhedral quartz phenocrysts are up to 1.5 mm in diameter, and igneous brown biotite is up to 1.5 mm in length. Plagioclase is euhedral and is up to 0.8 mm in length.

Igneous Geochemistry

The Mesozoic granitic rocks in the Pine Grove District all have undergone some degree of hydrothermal or metamorphic alteration. This causes difficulties in describing and characterizing the original igneous composition of the host rocks. Analyses in Table 2 and Appendix 4 give the major and trace element compositions of rock and alteration types from the Wheeler Mine area. Most of the major elements contents (i.e., K, Na, Fe, Ti, Al, Mn, Mg, and Ca) have been effected by hydrothermal alteration. Figure 4a and 4b are plots of total alkali content and K_2O content versus SiO_2 content for one sample of the granodiorite of Lobdell Summit (DSP 6) and two samples of the Wheeler granite porphyry (DSP 16 and 53). These samples were chosen because they were not strongly altered. The granodiorite of Lobdell Summit plots in the High K Dacite field of Ewart (1979) on the K_2O versus silica diagram and in the High Al field of Kuno (1959) on a plot of total alkalies versus silica diagram. The Wheeler granite porphyry samples plot in the alkalic field of Kuno (1959) on a plot of total alkalies versus silica diagram. The two porphyry samples plot in the High K Dacite field of Ewart (1979) near its upper boundary where Ewart's fields are undefined. Figure 5a and 5b are plots of P_2O_5 content and Zr content versus SiO_2 content for the Mesozoic granitic rocks

Table 2. Major Element Compositions of the Mesozoic Rocks in the Pine Grove District, Lyon County Nevada.

Rock Type	Jgd	Jgd	Jgd	Jgd	Jgd	Jgd	Jgd
Sample Number	DSP 6	DSP 8	DSP 39	DSP 55	DSP 57	DSP 60A	DSP 60AS
Unnormalized Results (wt.%):							
SiO_2	66.35	74.92	65.40	66.40	75.42	65.08	64.23
Al_2O_3	15.31	11.66	15.36	15.39	8.75	15.58	16.53
TiO_2	0.489	0.427	0.532	0.541	0.389	0.555	0.572
FeO^*	4.24	4.11	4.36	3.92	5.35	5.10	5.26
MnO	0.087	0.094	0.140	0.066	0.007	0.124	0.144
CaO	4.18	1.34	3.66	2.12	0.12	2.17	2.25
MgO	1.52	1.50	2.15	2.19	0.20	2.36	2.59
K_2O	3.01	3.20	0.64	2.77	3.25	2.35	2.89
Na_2O	3.28	0.58	6.25	4.45	0.64	4.62	3.59
P_2O_5	0.117	0.079	0.119	0.127	0.051	0.131	0.133
Total	98.58	97.73	98.61	97.97	94.18	98.07	98.19

Rock Type	Jgd	Jgp	Jgp	Jmd	Jm	Jqp	Jhp
Sample Number	DSP 111	DSP 16	DSP 53	DSP 3	DSP 41	DSP 2	DSP 165
Unnormalized Results (wt.%):							
SiO_2	66.89	68.54	67.99	59.08	62.02	75.11	64.07
Al_2O_3	15.89	14.71	14.82	18.02	19.15	13.86	16.69
TiO_2	0.454	0.332	0.361	0.712	0.169	0.188	0.560
FeO^*	3.83	2.84	2.96	6.00	1.22	1.34	3.76
MnO	0.089	0.022	0.025	0.050	0.038	0.006	0.028
CaO	1.44	1.56	2.34	1.24	2.33	0.29	1.62
MgO	1.60	0.96	1.05	1.73	0.80	0.23	1.43
K_2O	2.52	4.75	4.61	3.94	4.86	0.32	0.15
Na_2O	5.91	4.12	3.55	7.61	6.93	8.18	10.01
P_2O_5	0.112	0.112	0.121	0.403	0.013	0.051	0.259
Total	98.73	97.95	97.83	98.82	97.53	99.58	98.58

FeO^* is where Fe is calculated as Fe^{2+}

Samples DSP 6, DSP 8, 39, 55, 57, 60A, 60AS, and 111 are samples of granodiorite of Lobdell Summit. DSP 6 has been metamorphically altered. DSP 55, DSP 60A, and DSP 111 are altered to a Potassic-Sodic 4 assemblage. DSP 60AS is a sample of a quartz-sulfide vein selvage in granodiorite altered to Potassic-Sodic 4 assemblage. DSP 57 is altered to a quartz-sericite assemblage. DSP 8 is altered to a moderate sericitic assemblage.

DSP 3 is a sample of microdiorite altered to Potassic-Sodic 4 assemblage.

DSP 41 is a sample of monzonite altered to Potassic-Sodic 3 assemblage.

DSP 16 and 53 are samples of Wheeler granite porphyry altered to Potassic-Sodic 2 assemblage.

DSP 2 is a sample of quartz porphyry altered to Sodic 1 assemblage.

DSP 165 is a sample of hornblende granite porphyry altered to Sodic 2 assemblage.

Figure 4a.

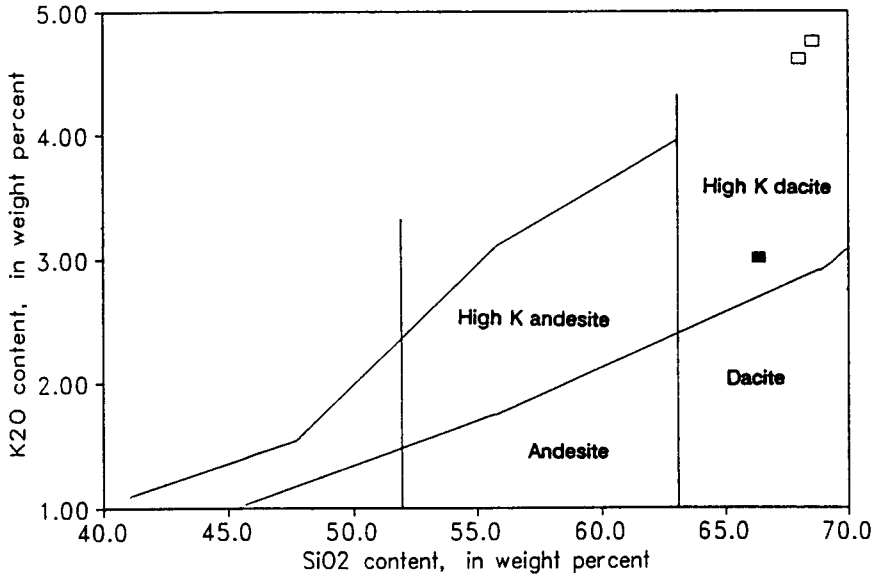

Figure 4b.

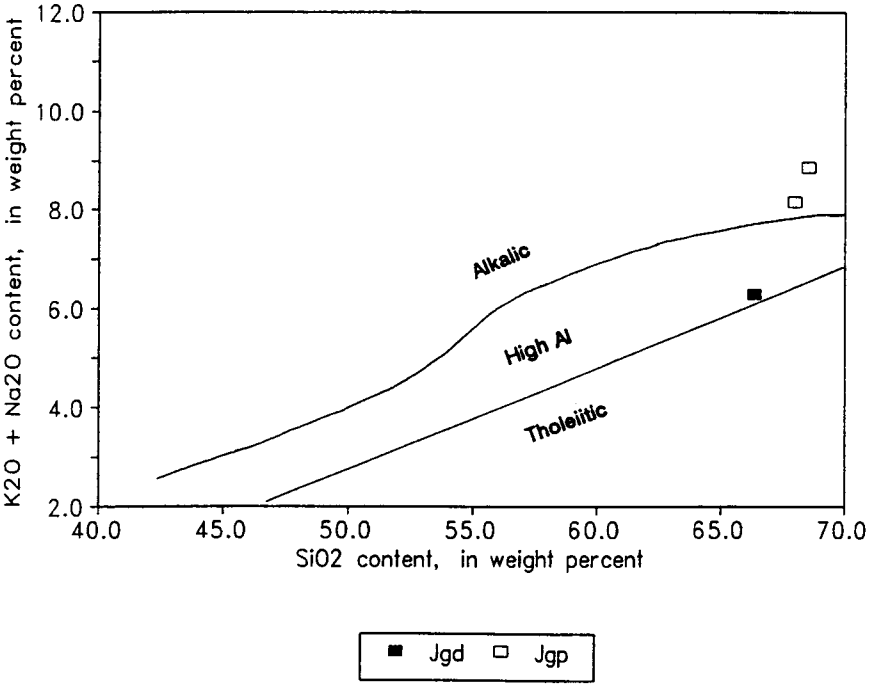

Figure 4. Plots of K_2O and K_2O + Na_2O content versus SiO_2 content for the least hydrothermally altered samples of Mesozoic granitic rocks.

Figure 5a.

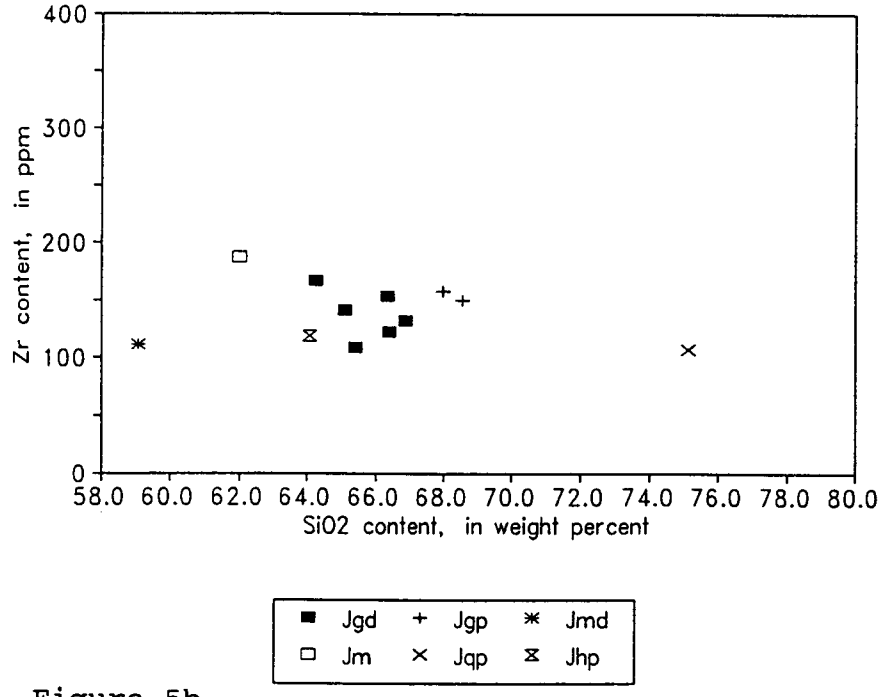

Figure 5b.

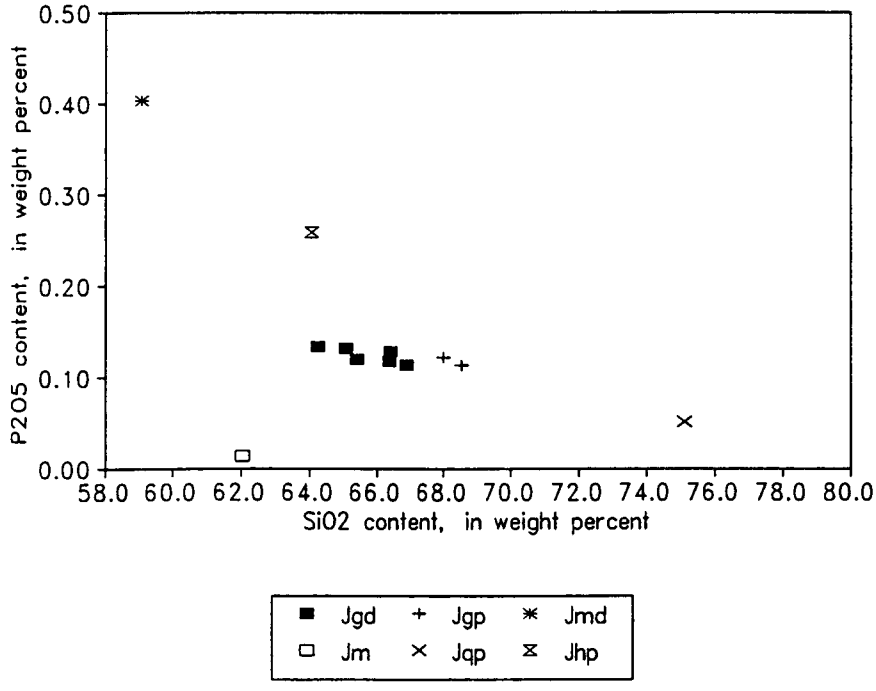

Figure 5. Plots of P_2O_5 content and Zr content versus SiO_2 content for the Mesozoic granitic rocks.

in the Wheeler Mine area. These diagrams indicate that with increasing silica content there is a decrease in the P_2O_5 content and possibly a slight decrease in Zr contents of the granitic rocks. Two samples (DSP 8 and 57) of the granodiorite of Lobdell Summit were not plotted because they have been altered so strongly that silica has been added to the samples; however, the remaining samples probably had little addition or loss of P, Zr, and SiO_2, particularly since P_2O_5 and Zr are relatively immobile during alteration.

Chondrite-normalized trace element plots for the Mesozoic granitic rocks and alteration types are shown on Figures 6a and 6b. C1 chondrite values from Anders and Ebihara (1982) were used with the mass of carbon and water subtracted. Figure 6a is a plot of least altered samples of granodiorite of Lobdell Summit, Wheeler granite porphyry, and monzonite from the Wheeler Mine area. Figure 6b is a plot of all granitic rock types for the Wheeler Mine area. All samples of the microdiorite, quartz porphyry, and hornblende granite porphyry in the Wheeler Mine area have undergone strong alteration. The least altered Mesozoic granitic rocks have essentially the same pattern for trace elements. The samples have the typical pattern of calc-alkaline rocks from island arcs (Jakes and Gill, 1970). All the rocks show a moderate enrichment (up to 100X chondrite values) of light rare earth element (REEs) with a pattern sloped towards lower abundances at higher atomic numbers.

Figure 6a.

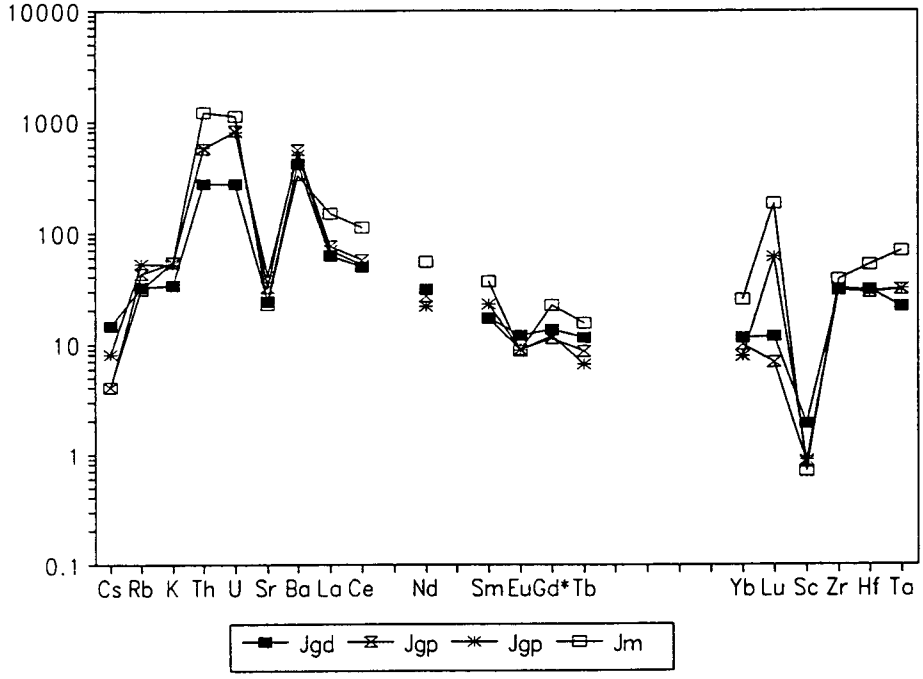

Figure 6b.

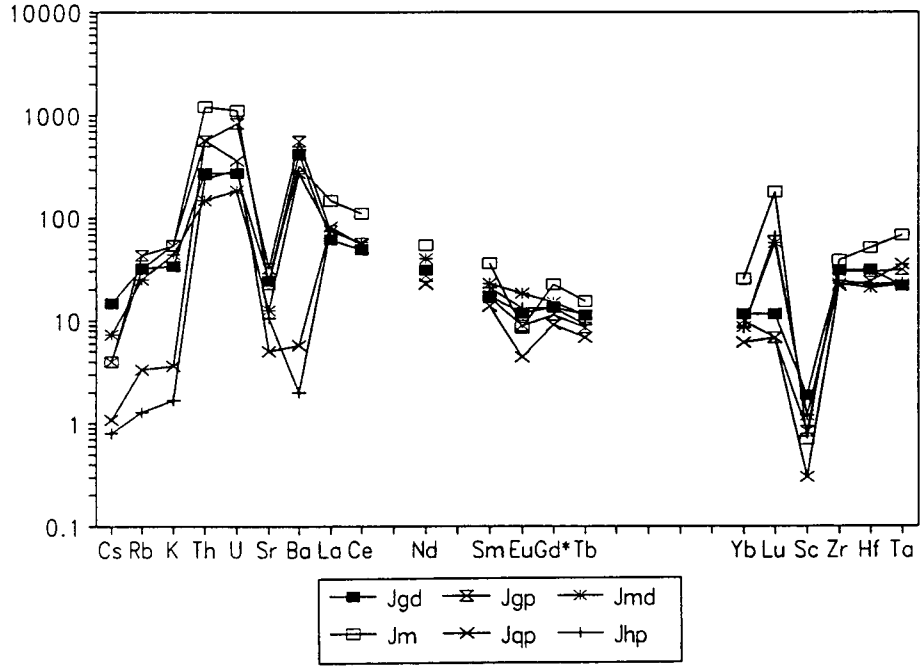

Figure 6. C1 chondrite normalized trace element plots for the Mesozoic granitic rocks (C1 chondrite values of Anders and Ebihara, 1982). Figure 6a is a plot of least hydrothermally altered samples and Figure 6b is a plot of each rock type from the Mesozoic rocks.

The heavy REEs are not as enriched (10X chondrite values) and have nearly a flat pattern. All samples are very enriched in Th and U, and are depleted in Sc and Sr. The Mesozoic rocks also have similar concentrations of high field strength, incompatible elements (i.e. Zr, Hf, Ta). Some of the more significant differences, particularly in the Quartz Porphyry and Hornblende Granite Porphyry, are due to the strong hydrothermal alteration. These two porphyries have undergone strong sodic alteration which has removed Cs, Rb, K, Sr, and Ba (Figure 6b).

The main minerals of the granodiorite of Lobdell Summit and the later granitic intrusions are plagioclase, microcline or orthoclase, quartz, hornblende, and biotite with minor and trace amounts of apatite, titanite, magnetite, and allanite. The presence of hornblende indicates that there was >4 weight percent water in the magma (Burnham, 1979).

Electron microprobe analyses of allanite and titanite (Appendices 2 and 3) and a instrumental neutron activation analysis of a whole rock from the granodiorite of Lobdell Summit are normalized to C1 chondrite values (Anders and Ebihara, 1982) and are plotted on Figure 7. Allanite is more enriched in light REEs, and titanite is more enriched in the heavier REEs than the whole rock. The allanite has 200-300X the concentrations of Th and Sm as the whole rock, and it has 1000X the concentrations of La, Ce, and Nd as the whole

Figure 7.

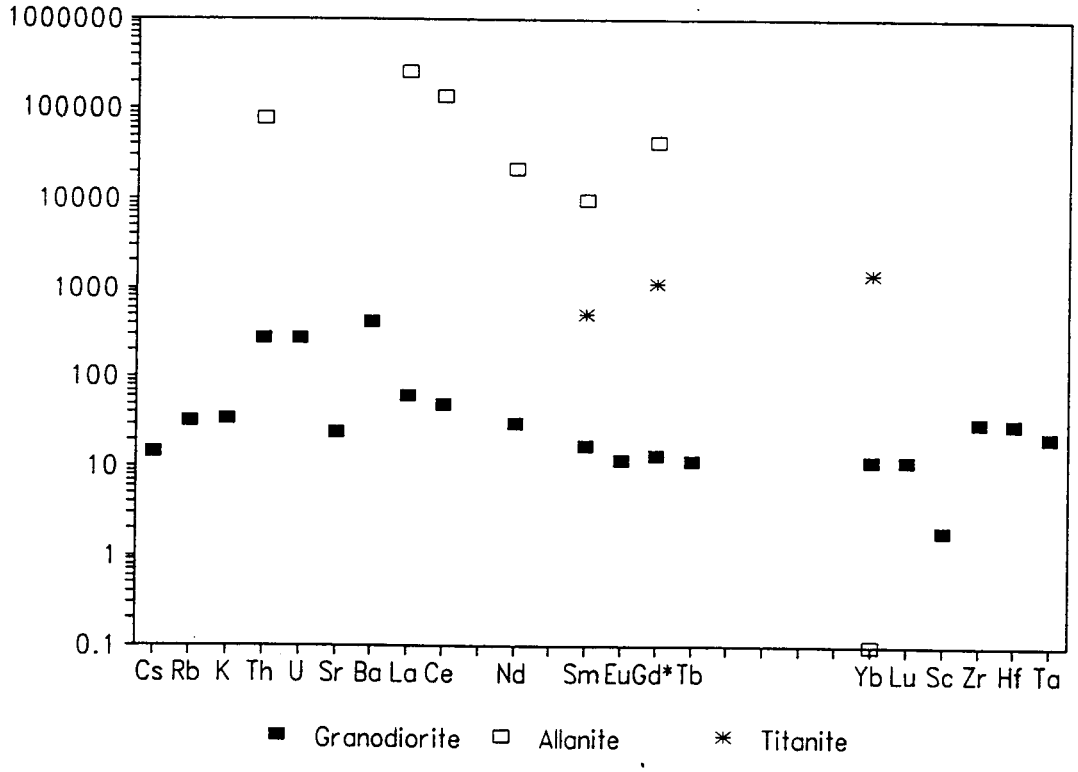

Figure 7. C1 chondrite normalized trace element plot of allanite, titanite, and the granodiorite of Lobdell Summit (C1 chondrite values of Anders and Ebihara, 1982).

rock. Titanite has 100X the concentrations of Sm and Yb, but less than 100X the concentrations of other REEs and Th as the whole rock. The light REEs of the allanite have the same abundance pattern as the light REEs of the granodiorite. Titanite has a flat heavy REE pattern, and this is similar to flat heavy REE pattern of the whole rock. In other granites documented (Gromet and Silver, 1983; Suzuki and others, 1990), allanite and titanite contain up to 80-95% of REEs present in the whole rock. Attempts by the author failed to determine the contributions of allanite and titanite in the granodiorite to the whole rock REE values due to difficulties in determining the volume percents of the minerals. Back calculations indicate that if allanite had a volume percent of 0.025 it could account for the lighter REE and Th concentrations in the granodiorite. The back calculations for titanite are very crude due to very low levels of REEs present, but if the titanite had a volume percent of approximately 0.7-0.8 it could account for the heavier REEs in the granodiorite. These calculated modes are not unreasonable in view of the modal observations (Table 1).

Figures 8a and 8b are plots of Al cations versus Ti cations and (Na+K+Al)/4 versus Fe/(Fe+Mg) for amphiboles from the granodiorite of Lobdell Summit (Jgd) and hornblende granite porphyry (Jhp). Two populations are apparent on the diagrams with the hornblende from the granodiorite having

Figure 8a.

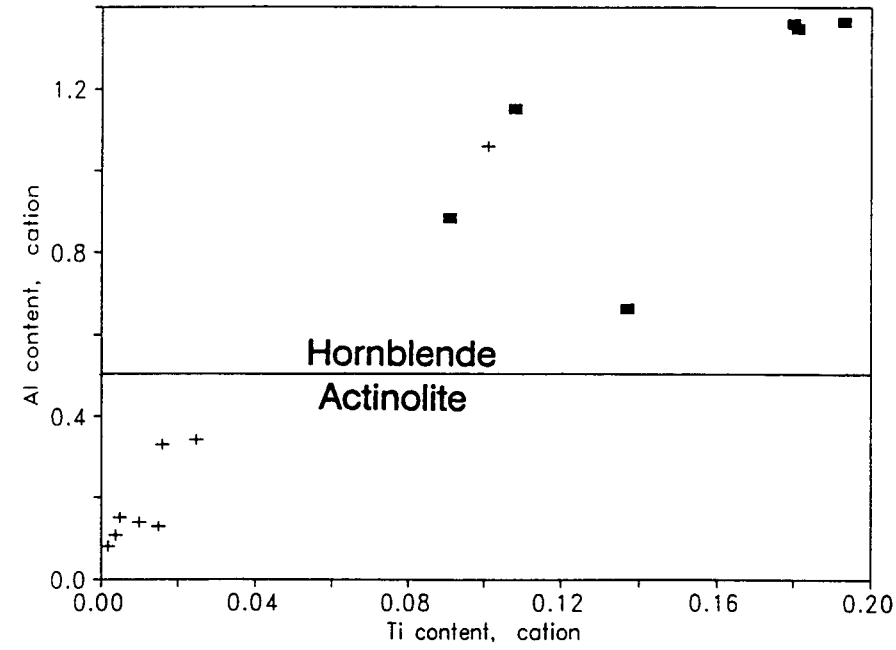

Figure 8b.

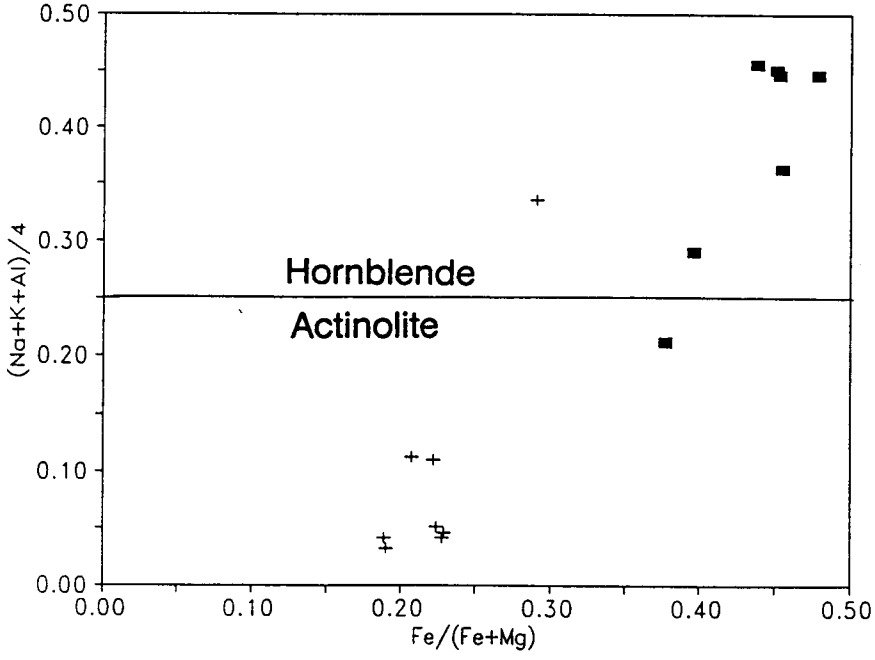

Figure 8. Plots of total Al versus Ti and (Na+K+Al)/4 versus Fe/(Fe+Mg) for amphiboles from the granodiorite of Lobdell Summit (Jgd) and the hornblende granite porphyry (Jhp).

greater amounts of Al, Ti, Fe, and alkalies than the actinolite from the porphyry (Table 3). One analysis of amphibole in the hornblende granite porphyry indicates that there is still a trace amount of igneous hornblende remaining. The original igneous amphibole in the hornblende granite porphyry is similar to the amphibole in the granodiorite of Lobdell Summit, but it has a smaller Fe/(Fe+Mg) ratio than the amphibole in granodiorite. Igneous hornblende has a Fe/(Fe+Mg) ratio of 0.41 to 0.47 in the granodiorite, and the igneous hornblende in the hornblende granite porphyry has a Fe/(Fe+Mg) ratio of 0.29. The low totals for hornblende analyses (Table 3) are probably due to iron in the amphiboles being largely Fe^{3+} instead of Fe^{2+} which could increase the totals by as much as 1.6 wt.%. Using Leake's (1978) classification system for amphiboles, the amphiboles in the granodiorite of Lobdell Summit would be classified as actinolitic hornblende, whereas the amphibole from the hornblende granite porphyry would be classified as actinolite.

Estimates for the pressure of crystallization of the granodiorite of Lobdell Summit can be calculated using the total aluminum content of the hornblende. The granodiorite has the appropriate assemblage for a pressure estimate: microcline, quartz, plagioclase, hornblende, biotite, magnetite, and a Ti phase (Hammarstrom and Zen, 1986). The Hammarstrom and Zen (1986) geobarometer equation,

Table 3. Electron Microprobe Analyses of Amphiboles

Rock Type								
Sample Number	DSP 201				DSP 165			
Mineral Wt.%	Hbl	Hbl	Hbl	Hbl	Act	Act	Act	Act
SiO_2	45.48	46.14	49.02	45.36	53.88	56.59	55.76	56.72
TiO_2	1.69	1.69	0.80	1.56	0.14	0.02	0.10	0.04
Al_2O_3	7.61	7.63	5.00	7.50	1.95	0.48	0.83	0.65
MgO	11.41	10.92	12.92	10.99	18.16	19.26	18.18	19.46
CaO	10.66	10.81	10.85	10.84	12.23	12.48	12.76	12.13
MnO	0.71	0.81	0.98	0.77	0.17	0.08	0.18	0.11
FeO	15.87	16.15	15.09	16.12	9.23	8.06	9.64	8.08
Na_2O	1.12	1.06	0.72	1.13	0.34	0.14	0.13	0.21
K_2O	0.64	0.57	0.35	0.58	0.07	0.04	0.05	0.02
H_2O*	1.97	1.98	2.00	1.95	2.08	2.13	2.12	2.13
Total	97.16	97.78	97.74	96.80	98.26	99.29	99.74	99.56
(Na+K+Al)/4	0.43	0.42	0.27	0.45	0.11	0.03	0.04	0.04
Fe/(Fe+Mg)	0.44	0.45	0.40	0.46	0.22	0.19	0.23	0.19
Total Al	1.37	1.36	0.88	1.36	0.33	0.08	0.14	0.11

* Calculated by stoichiometry assuming Σ cations equals 23 with 2(OH^-) replacing a O^{2-}

$P= -3.92+5.03Al_t$, gives a pressure range of 2.85 to 2.97 kilobars. The Hollister and others (1987) geobarometer equation, $P= -4.76+5.64Al_t$, gives a pressure range of 2.83 to 2.96 kilobars. The Johnson and Rutherford (1989) geobarometer equation, $P= -3.46+4.23Al_t$, gives a pressure range of 2.23 to 2.33 kilobars. These pressures correspond to 7-10 kilometers of depth of emplacement.

Igneous and secondary biotite compositions from the Mesozoic granitic rocks in the Wheeler Mine area have TiO_2 contents generally between 0.5 to 1.5 wt.% and a Fe/(Fe+Mg) ratio between 0.37 to 0.55 (Figure 9, Appendix 5)). All the biotite analyzed in the Pine Grove District came from rocks that had undergone minor to extensive hydrothermal alteration and likely were later metamorphosed (see discussion below). The TiO_2 content for these biotites is low compared to biotites from other porphyry deposits. The TiO_2 content of biotite at Santa Rita, New Mexico, ranges from 2.2 to 4.5 wt.% (Jacobs and Parry, 1979), at Bingham, Utah, ranges from 1.6 to 6.0 wt.% (Moore and Czamanske, 1973; Parry and others, 1978), and at Yerington, Nevada ranges from 1.3 to 4.2 wt.% (Carten, 1986; Dilles, 1987). The low TiO_2 content of the Pine Grove District biotites could be due to the exsolution of TiO_2 from the biotite during hydrothermal alteration by fluids as described elsewhere (Lanier and others, 1978) and is supported by the presence of sagenitic rutile. The low TiO_2 content could

Figure 9.

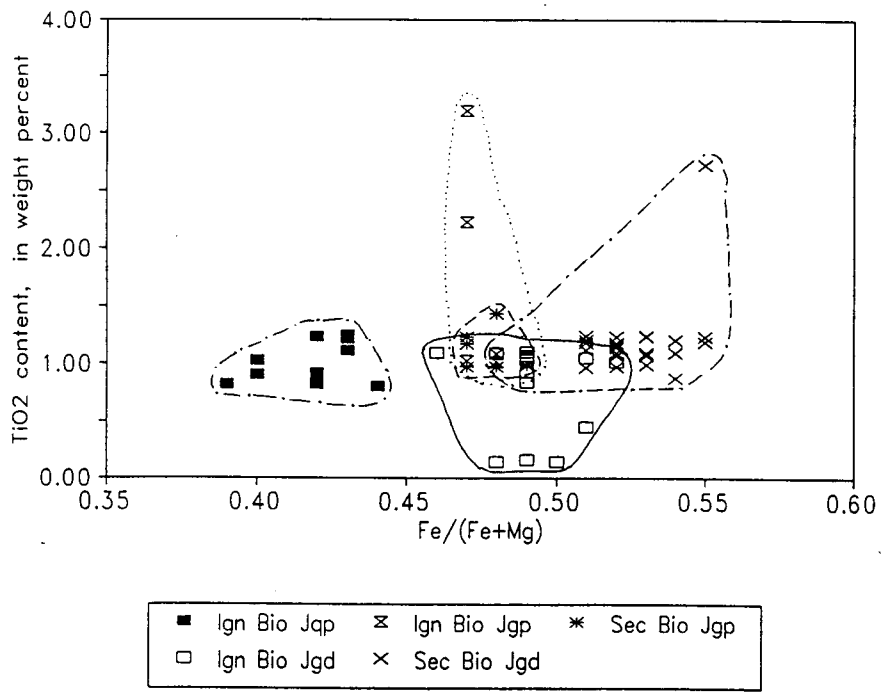

Figure 9. Plot of TiO_2 content versus Fe/(Fe+Mg) for biotite from the Pine Grove District, Lyon County Nevada.

also be due to later low temperature metamorphism. Several biotite analyses from the Pine Grove rocks had higher than average TiO_2 contents. These high TiO_2 analyses were from the cores of biotite grains and may represent only partial exsolution of TiO_2. Other analyses on the rims of these biotite grains had the typical low TiO_2 values. The TiO_2 content of the biotite at Pine Grove District is not affected by the presence or absence of magnetite as it is at the nearby Yerington deposit (Dilles, 1984). The secondary biotite at the Wheeler Mine has a lower Mg content and higher Fe/(Fe+Mg) ratio than the primary biotite. This is not the same trend found at other porphyry deposits (i.e., Santa Rita and Bingham). This is illustrated well on Figure 9 where the secondary biotite in the granodiorite of Lobdell Summit (Jgd) has a higher Fe content than the primary biotite present. The primary biotite and secondary biotite in the Wheeler granite Porphyry (Figure 9, Jgp) have similar TiO_2 content and Fe/(Fe+Mg) ratios and are generally more Mg-rich than the biotite from the granodiorite. The biotite from the quartz porphyry (Figure 9, Jqp) has about the same TiO_2 as other biotites in the district, but is much more Mg-rich than other biotites present. This could be a reflection of the intensity of alteration as the granodiorite of Lobdell Summit and Wheeler granite porphyry are less altered than the quartz porphyry. The Mg content of the biotite at

Bingham (Lanier and others, 1978) increases with intensity alteration.

Discussion of Igneous Geochemistry

All the Mesozoic granitic rocks in the Pine Grove District are interpreted to be genetically related and the result of the one period of magmatism due to their similar REE patterns (Figures 6a and 6b). This magmatism was calc-alkaline in nature, and the Pine Grove granitic rocks may be the plutonic equivalents of high K arc andesites and dacites. Differentiation of a calc-alkaline magma probably produced the series of major intrusions (i.e. Wheeler granite porphyry, quartz porphyry) at the Pine Grove District. Progressing from oldest to youngest, the major intrusions become more silica-rich and potassium rich, and richer in incompatible trace elements.

These granitic rocks are probably related to a period of late Triassic-early Jurassic magmatism in the region that was characterized by accessory allanite. All of the Mesozoic granitic rocks in the Pine Grove District contain allanite in trace amounts, and J.H. Dilles and D.A. John (personal commun., 1993) have found allanite in other deformed plutons of similar age in the region.

The Mesozoic granitic rocks intruding the granodiorite of Lobdell Summit are sharp-walled dikes that have strikes

of north to northwest. Cross-cutting relationships between the dikes indicate that the dikes were emplaced as several events. The major dikes through time become coarse-grained and volumetrically smaller.

The hornblende geobarometer results indicate that the granodiorite of Lobdell Summit was emplaced at a paleodepth of 7-10 kilometers. This depth of emplacement is compatible with a minimum paleodepth of 3-4 kilometers at the Wheeler Mine based the thickness of the overlying granodiorite, tilted 50-60° W in the present cross-sectional view (Figure 3). There is no indication that after the emplacement of the granodiorite of Lobdell Summit that it was uplifted significantly prior to the emplacement of the granitic dikes, so it is assumed that dikes were emplaced at a similar depth.

The magmas for the Mesozoic plutonic rocks had significant water contents. The presence of hornblende in these rocks indicates that there were >4 weight percent water in the melts (Burnham, 1979). Also, the porphyritic texture of dikes indicates that there was significant water present in magmas. The granite porphyry dikes are characterized by abundant phenocrysts (> 1 mm) set in a fine-grained (< 0.01 mm) aplitic or graphic groundmass. Experimental studies of hydrous granite melts have shown that the escape of the volatiles (water) causes a pressure

quench of the granitic melt to form the aplitic and graphic groundmass textures (Swanson and Fenn, 1986).

Biotite compositions in the district may reflect metamorphic alteration since they do not have the expected trend of secondary biotite having higher Mg contents than the primary biotite by comparison to well-studied porphyry copper deposits. The metamorphic alteration partially recrystallized the secondary biotite into a poorly developed foliation, and this may have changed the Mg/(Fe+Mg) ratio of the biotite.

The Mesozoic granitic dikes are spatially and temporally related to hydrothermal alteration and mineralization. The Wheeler granite porphyry, microdiorite, and monzonite dikes were emplaced before potassic alteration took place, and the quartz porphyry and hornblende granite porphyry dikes were emplaced afterwards. Since all these dikes have similar trace element patterns that are similar to the granodiorite of Lobdell Summit, the period of dike emplacement and hydrothermal activity is near the age of the granodiorite of Lobdell Summit as given by Rb-Sr isochrons: 186.9±8.5 Ma (John and others, 1991; 186.5±7.7 Ma (Robinson and Kistler, 1986).

ALTERATION AND MINERALIZATION

The hydrothermal alteration and mineralization at the Wheeler Mine is complex because younger hydrothermal events overprint older ones, a metamorphic event overprints the hydrothermal events, and Tertiary deformation has displaced and deformed rocks from higher in the hydrothermal system next to those from lower across the Stonehouse Fault. Due to later hydrothermal events overprinting the potassic alteration, most of the rocks in the Wheeler Mine area have a Mixed Series assemblage: Mixed Series assemblages are a combination of potassic alteration and sodic alteration as described below.

Potassic Alteration

Distribution and Age

Potassic alteration is interpreted to be the earliest hydrothermal alteration event at the Wheeler Mine. Potassic alteration is older than sodic alteration because actinolite veins associated with sodic alteration cut and offset biotite veinlets associated with potassic alteration. This relationship is also suggested by the hornblende granite porphyry containing sodic alteration but not potassic alteration; hence the hornblende granite porphyry dikes were

emplaced after potassic alteration. There is also the possibility that there were two sodic alteration events, but there is no certain evidence for it. Potassic alteration is older than sericitic alteration because biotite veinlets are cut and offset by veins with sericitic selvages.

Due to later hydrothermal alteration events overprinting the early potassic assemblage, there is only one potassic assemblage preserved in the mine area: moderate potassic. The moderate potassic assemblage is present in several areas west of the Stonehouse Fault and east of the metamorphic assemblage (Plates 3 and 4). Most areas containing the moderate potassic assemblage are west of the Wheeler granite porphyry dike, but there are a few exceptions. One area containing the moderate potassic assemblage is just east of the Stonehouse Fault around the 6600 level adit entrance (Plate 1). This block is interpreted to be faulted into place by the Stonehouse Fault. Another area containing the moderate potassic assemblage is the large block of granodiorite of Lobdell Summit in the Wheeler granite porphyry (Plate 1). This block of granodiorite, too, is thought to be faulted into place, but no fault is apparent on the surface.

Potassic Assemblage

Potassic alteration at the Wheeler Mine is characterized by magmatic minerals being replaced by hydrothermal biotite. This secondary biotite has a shreddy texture. Shreddy texture is defined as randomly oriented aggregates of fine-grained, subhedral flakes. In the moderate potassic assemblage (Table 4, Plates 3 and 4), secondary biotite totally replaces magmatic hornblende, and some (generally less than 5%) calcic plagioclase is lightly dusted with biotite. Rutile is present in biotite cleavages due to exsolution from biotite during hydrothermal alteration. Igneous hornblende, andesine, microcline, biotite, magnetite and ilmenite are still present in this assemblage. There is no sulfide mineralization associated with this assemblage.

Later alteration has also affected this assemblage. It has lightly dusted all plagioclase with fine-grained sericite. Trace amounts of epidote also replace plagioclase grains and chlorite replaces trace amounts of biotite. The moderate potassic assemblage (Table 4, Plates 3 and 4) differs from the metamorphic assemblage primarily by all of the igneous hornblende being altered to hydrothermal biotite.

Table 4. Hydrothermal Alteration Assemblages at the Wheeler Mine , Pine Grove District, Lyon County Nevada.

Alteration Type	New and Recrystallized Minerals	Relict Minerals
Potassic:		
Moderate potassic	Bio + Ep + (Ser) ± (Chl) + (Rut)	And + Ksp + Ign Bio + Mag + (Ti) + (Ilm)
Sodic:		
Sodic 1	Alb + Chl ± (Ep) + (Rut)	Ign Bio
Sodic 2	Alb + Act + Chl + Mag	Mag + (Ign Bio)
Mixed Potassic-Sodic Series:		
Potassic-Sodic 1	Bio + Ep + Alb + Olg + (Ser) + (Chl) + (Rut)	Ksp + Hbl + Ign Bio + Mag + (Ti) + (Ilm)
Potassic-Sodic 2	Bio + Ep + Alb + Olg + (Ser) + (Rut) ± (Chl) ± (Ti)	Ksp + Ign Bio + Mag + (Ti)
Potassic-Sodic 3	Bio + Alb + Olg + Ep + (Ser) + (Rut) ± (Chl)	Ign Bio + Mag
Potassic-Sodic 4	Bio + Alb + Olg + Ep + (Rut) + (Chl) + Qtz	± (Ign Bio) + Mag
Potassic-Sodic 5a	Act + Qtz +(Chl) ± (Ep)	
Potassic-Sodic 5b	Act + Chl + (Ep)	Ign Bio + Hyd Bio + Olg + Alb + (Rut) + (mag) ± (Cp) ± (Py)
Sericitic:		
Quartz-Sericite	Qtz + Ser + Py>>Cp ± (Alb)	
Weak Sericitic	Ser + Alb ± (Qtz) ± (Chl) ± (Py)	Ign Bio + Hyd Bio + (Mag)
Metamorphic:		
Weak biotitization	Bio + Ep + (Ser) + (Chl) + (Rut)	And + Ksp + Hbl + Ign Bio + Mag + (Ti) + (Ilm)

Abbreviations are in Appendix 6.

Veins

There are only two types of veining in the potassic assemblage: biotite and epidote (Table 5). The biotite veinlets do not have any apparent selvages, are not over 1 mm wide, and are cut and offset by epidote veins. The biotite veinlets are very rare in the moderate potassic assemblage with a density up to 1%, but typically much less.

The epidote veins consist of epidote with trace amounts of quartz and possibly chlorite and pyrite. The epidote veins are most likely part of the sodic alteration, which has actinolite veins with selvages in which biotite has been altered to chlorite. The epidote veins are typically 2-5 mm wide and have selvages that consist of biotite altered to chlorite and plagioclase replaced by minor amounts (1-5%) of epidote. These selvages extend up to 10 mm outward from a vein. The epidote veins can have densities as high as 5%, but they generally have densities much less than 1%.

Sodic Alteration

Distribution and Age

Sodic alteration is younger than potassic alteration as described above, and it is older than sericitic alteration. Veins with sericitic selvages cut rock that has undergone

Table 5. Vein Assemblages at the Wheeler Mine, Pine Grove District, Lyon County Nevada.

Vein Type	Mineral Present in Vein	Minerals in Selvage(s)
Biotite Veins	Bio	no selvage present (in pervasive potassic alteration)
Act-Qtz Veins	Act ± Qtz	Olg + Act + Chl ± (Ep) (inner) // Act + Chl ± (Ep) (outer)
Epidote Veins	Ep ± (Qtz) ± (Chl) ± (Py)	Ep + Chl
Barren Quartz Veins	Qtz ± Chl ± Py	Chl
Qtz-Sulfide Veins	Qtz ± (Cp) ± (Py) ± (Mc) ± (Mag) ± (Po) ± (Native Au)	Ser + Alb ± (Chl)
Cp-Py Veins	Cp + Py ± Qtz ± (Mc)	Ser + Alb ± (Chl)
Pyrite Veins	Py ± Qtz	Ser + Alb

Abbreviations are in Appendix 6.

sodic alteration. However, no veins with sericitic selvages were observed cutting and offsetting veins associated with sodic alteration.

There are two sodic alteration assemblages (Table 4) in the Wheeler Mine area. The sodic 1 assemblage occur only in the quartz porphyry dikes and the sodic 2 assemblage only occurs in the hornblende granite porphyry dikes (Plates 3 and 4).

Assemblages

Both sodic assemblages are largely characterized by potassium feldspar (microcline or orthoclase) that has been replaced by hydrothermal albite. The potassium feldspar that has been altered to albite has the characteristic short, irregular twins of hydrothermal albite described elsewhere (Gilluly, 1933; Carten, 1986). Figure 10a and 10b are photomicrographs of such secondary albite. In the sodic 1 (albite-chlorite) assemblage (Table 4, Plates 3 and 4), potassium feldspar and magmatic plagioclase have been altered to albite, and igneous biotite has been partially altered to chlorite. Trace amounts of epidote replace what were originally magmatic plagioclase phenocrysts, and rutile is present in biotite cleavages due to exsolution from biotite during hydrothermal alteration.

Figure 10. Photomicrographs of illustrating the twinning in secondary albite. In Figure 10a, secondary albite has replaced a large potassium feldspar phenocryst which has magmatic plagioclase inclusions. The fine-grained groundmass of quartz + potassium feldspar in the quartz porphyry has been altered to quartz + albite. Figure 10b is a grain of microcline in the granodiorite of Lobdell Summit that has been replaced by secondary albite. Note the randomly orientated secondary biotite which has replaced magmatic hornblende.

Figure 10a.

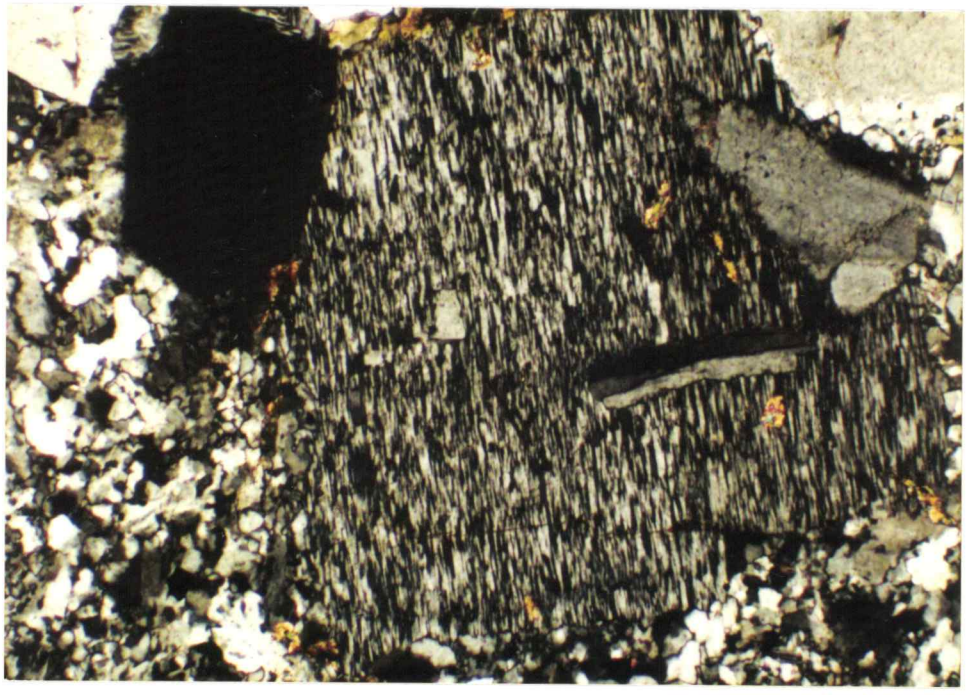

Figure 10b.

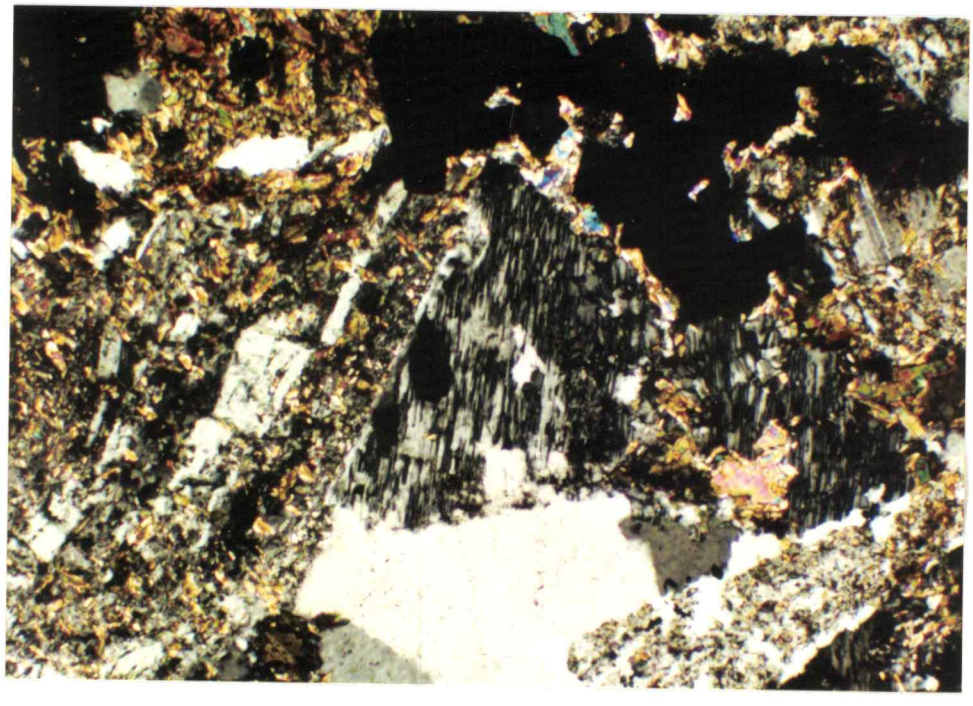

The sodic 2 (albite-actinolite-chlorite) assemblage (Table 4, Plates 3 and 4) is similar to the sodic 1 assemblage in that potassium feldspar and magmatic plagioclase have been altered to albite, and igneous biotite has been partially altered to chlorite.

Sodic 2 assemblage differs from the sodic 1 assemblage because it contains actinolite and magnetite that have replaced igneous hornblende. This difference between the two sodic assemblages is probably a reflection of the original hostrock compositions. The sodic 2 assemblage occurs only in the hornblende granite porphyry, which originally contained 7-8% magmatic hornblende, and the sodic 1 assemblage occurs only in the quartz porphyry, which did not have any magmatic hornblende to be altered to actinolite.

The sodic 1 and 2 assemblages do not have any veining associated with them.

Mixed Potassic-Sodic Assemblages

Distribution

The mixed potassic-sodic assemblages reflect a combination of potassic and sodic alteration due to overprinting of a early potassic hydrothermal event by a later sodic event as documented below. The mixed potassic-sodic assemblages 1 through 3 are located west of Stonehouse

Fault (Plates 3 and 4). The mixed potassic-sodic assemblages 1 and 3 occur in the granodiorite of Lobdell Summit, and the mixed potassic-sodic 2 assemblage occurs in the both the granodiorite of Lobdell Summit and Wheeler granite porphyry. The mixed potassic-sodic 4 and 5 assemblages occur between the Wheeler and Stonehouse Faults in the granodiorite of Lobdell Summit (Plates 3 and 4).

Assemblages

The potassic-sodic 1 assemblage (Table 4, Plates 3 and 4) is characterized by the partial replacement of magmatic hornblende by hydrothermal biotite and the partial replacement of potassium feldspar (microcline) by hydrothermal albite. The secondary biotite has a shreddy texture, and the hydrothermal albite has the characteristic short, irregular twins described elsewhere (Gilluly, 1933; Carten, 1986). This assemblage probably represents the overprinting of sodic alteration by the metamorphic event. There are about 5% biotitized plagioclase grains present, and igneous plagioclase is altered to oligoclase and is no longer zoned. Rutile is present in biotite cleavage due to exsolution from biotite during hydrothermal or metamorphic alteration. Trace amounts of plagioclase are altered to epidote, and trace amounts of biotite are altered to chlorite. There is no sulfide mineralization associated with

this assemblage. There is relict magmatic hornblende, biotite, potassium feldspar, magnetite, titanite, and ilmenite remaining.

A later alteration event has lightly dusted magmatic plagioclase grains with fine-grained sericite in the potassic-sodic 1 assemblage.

Potassic-sodic 2 assemblage (Table 4, Plates 3 and 4) is characterized by hornblende replaced 100% by hydrothermal biotite and potassium feldspar partially replaced by hydrothermal albite. This assemblage is similar to potassic-sodic 1 assemblage in other respects. There is more biotitized plagioclase present, typically 3-7%. Secondary titanite is also present with biotite replacing igneous hornblende. Trace amounts of plagioclase have been altered to epidote and trace amounts of biotite are altered to chlorite. There is no sulfide mineralization associated with this assemblage. Relict igneous biotite, potassium feldspar, and magnetite remain in this assemblage.

A later alteration event has also lightly dusted magmatic plagioclase grains with fine-grained sericite in the potassic-sodic 2 assemblage.

The potassic-sodic 3 assemblage (Table 4, Plates 3 and 4) is characterized by hornblende being replaced 100% by hydrothermal biotite and potassium feldspar replaced 100% by secondary albite. This assemblage is similar to the potassic-sodic 1 and 2 assemblages in other respects. This

assemblage has more biotitized magmatic plagioclase grains, typically 5-15%, than the previous assemblages. Trace amounts of epidote also replace the magmatic plagioclase grains, and trace amounts of biotite are altered to chlorite. There is no sulfide mineralization associated with this assemblage. Relict igneous biotite and magnetite are still present in this assemblage.

A later event has lightly dusted magmatic plagioclase grains with sericite in the potassic-sodic 3 assemblage.

The potassic-sodic 4 assemblage (Table 4, Plates 3 and 4) is characterized by hornblende replaced 100% by hydrothermal biotite and potassium feldspar replaced 100% by hydrothermal albite as in potassic-sodic 3 assemblage. In the potassic-sodic 4 assemblage however, magmatic plagioclase grains are not lightly dusted with fine-grained sericite as in potassic-sodic 1-3 assemblages (with exception of vein selvages). Magmatic plagioclase has been altered to oligoclase and is no longer zoned. Plagioclase grains may also be replaced by trace amounts of epidote. Variable amounts of the magmatic plagioclase have been partially replaced by hydrothermal biotite. The amount of plagioclase grains replaced can be as low as 5% of total plagioclase grains present or as high as 80%. Generally, only 30-40% of the plagioclase present are affected. Trace amounts of igneous biotite are present, and this biotite has rutile in its cleavages due to exsolution from biotite

during hydrothermal alteration. Variable amounts of chlorite have replaced secondary and igneous biotite.

The potassic-sodic 5a and 5b assemblages are difficult to distinguish in the field so they are plotted as a combined potassic-sodic 5 assemblage on Plate 3. In the potassic-sodic 5a (oligoclase-actinolite) assemblage (Table 4), igneous and secondary biotite (remnants have the shreddy texture described above) is altered to actinolite with minor amounts of chlorite. Magmatic plagioclase is not zoned, and potassium feldspar has been altered to oligoclase. Trace amounts of epidote also replace the plagioclase. The potassic-sodic 5b assemblage is more a gradational assemblage between the potassic-sodic 5a assemblage and the potassic-sodic 4 assemblage. In the potassic-sodic 5b assemblage, igneous and secondary biotite is only partially altered to actinolite and/or chlorite. Plagioclase is not zoned, and is altered to oligoclase. Microcline is altered to albite. Trace amounts of epidote replace what was originally igneous plagioclase. Rutile is present in the biotite cleavage due to exsolution from biotite during hydrothermal alteration.

Veins

The potassic-sodic assemblages have the most variety and number of vein types in the Pine Grove District. All the

potassic-sodic assemblages have biotite and epidote veins present. Biotite veinlets (Table 5) are the oldest and most common vein type present. Biotite veinlets do not have any apparent selvages and their numbers increase eastward from the potassic-sodic 1 assemblage to potassic-sodic 4 and 5 assemblages at the Wheeler Mine (Plates 3 and 4). In the potassic-sodic assemblage 1 and 2, biotite veinlets have typical densities of less than 1%, whereas in the potassic-sodic assemblages 4 and 5, biotite veinlets can have a densities up to 30%, but typically are 5-15%. Biotite veinlets are cut and offset by all other vein types at the Wheeler Mine. The epidote veins consist of epidote with trace amounts quartz and possibly chlorite and pyrite. Epidote veins (Table 5) are typically 2-5 mm wide and can have bleached selvages in which mafic minerals are altered to chlorite. Epidote veins have a selvage that consists of biotite altered to chlorite and plagioclase replaced by minor amounts (1-5%) of epidote. The density of epidote veins is typically less than 1%.

The potassic-sodic 4 and 5 assemblages have barren quartz veins present in them. The barren quartz veins (Table 5) are largely quartz with very trace amounts of chlorite. Barren quartz veins are granular in texture, up to 8 cm wide (generally much less), and can have a 2-3 mm selvage of chlorite. The barren quartz veins only cut and offset biotite veins. Hence they are interpreted to be associated

with the sodic alteration event, here superimposed on the earlier potassic alteration.

Actinolite veinlets are characteristic of the potassic-sodic 5 assemblages (Table 5). These veins are 2-3 mm wide and can be as numerous as 6-8 per 30 cm. The actinolite veinlets are composed of actinolite with minor amounts of quartz. The potassic-sodic 5a (oligoclase-actinolite) assemblage forms a inner selvage that is centimeters wide around the actinolite veinlets, and the potassic-sodic 5b (actinolite-chlorite) assemblage forms a outer selvage around the veinlets that is ten's of centimeters wide. The actinolite-quartz veins cut and offset biotite veinlets. There is no clear evidence of their age with respect to epidote veins or veins with sericite or chlorite selvages. They are interpreted to be associated with sodic alteration of previously potassically altered rocks in assemblage 5.

Transitional Vein Assemblages

Distribution and Age

The transitional vein assemblages are veins and vein selvages that reflect a transition from the earlier potassic and sodic assemblages to the later sericitic assemblages. These veins contain native gold and copper sulfide minerals

which neither the veins in potassic and sodic assemblages or in the sericitic assemblages contain. The transitional veins have narrow selvages containing minor hydrothermal chlorite + sericite + albite, whereas the veins in the sericitic assemblages have wide, pervasive quartz-sericite selvages.

The transitional veins are found between the Wheeler and Stonehouse Faults, and to a minor extent, below the Stonehouse Fault in the granodiorite of Lobdell Summit. The transitional veins occur only within zones of potassic-sodic 4 and 5 assemblages in the mine area. The age of the transitional veins is younger than the potassic and sodic alterations, and older than the sericitic alteration.

Veins

The transitional veins are composed of quartz-sulfide and chalcopyrite-pyrite veins. Quartz-sulfide veins (Table 5) are granular in texture, and are generally 2-3 cm wide, but rare veins can be up to 15 cm wide. The vein assemblage is quartz ± chalcopyrite ± pyrite ± marcasite ± magnetite ± pyrrhotite ± native gold. These veins have selvages of sericitized and albitized plagioclase that extend up to 10 cm out from the vein. The sericite generally replaces up to 30-40% of the plagioclase grains, but it can be greater. Igneous and hydrothermal biotite is stable in these selvages. These veins typically have densities between 5-

10%, but can be up to 20%. The metamorphic deformation and Tertiary faulting in the region has altered the original orientation of quartz-sulfide veins. The orientations of the quartz-sulfide veins are plotted on Plate 6, and the vein orientations are not parallel the Tertiary faults.

In these veins, chalcopyrite has inclusions of pyrite and marcasite, while pyrite has inclusions of pyrrhotite, chalcopyrite, and marcasite. Magnetite has inclusions of chalcopyrite, pyrite, and marcasite. Marcasite has only inclusions of pyrite.

The presence of biotite in these vein selvages is unusual, and it is believed to be due to a metamorphic event (described below) which overprints the district. I propose that the secondary and igneous biotite in selvages was partially altered to chlorite + phengitic sericite when the veins formed. The later metamorphic event altered the chlorite + phengitic sericite back to biotite + (muscovite) sericite again. The equation for this reaction from Miyashiro (1973) is:

$$2(KMg_{0.5}Al_2Si_{3.5}O_{10}(OH)_2) + 1/3(Mg_6Si_4O_{10}(OH)_8 = KAl_3Si_3O_{10}(OH)_2 + KMg_3AlSi_3O_{10}(OH)_2 + 7/3(SiO_2) + 4/3(H_2O)$$

Quartz-sulfide veins cut and offset biotite veins, but their age with respect to other vein types is unclear. They are cut, but not offset by pyrite veins and are interpreted

to be older than the pyrite veins associated with sericitic alteration.

Chalcopyrite-pyrite veins are not as common as pyrite veins (associated with sericitic alteration) in the potassic-sodic assemblages where they occur together. In chalcopyrite-pyrite veins, the ratio of chalcopyrite to pyrite is 1:1 to 1:3. These sulfide dominated veins also contain minor amounts of quartz and marcasite. Veins of chalcopyrite-pyrite are 2-4 mm wide and can have densities up to 15%, but they are usually much less (<1%). The chalcopyrite-pyrite veins have selvages of partially sericitized and albitized plagioclase that extends up to 3 cm out from the veins. The chalcopyrite-pyrite veins cut and offset biotite veinlets, but their age with respect to other vein types is unclear.

Sericitic Alteration

Distribution and Age

The sericitic assemblages (Table 4) occur between the Wheeler and Stonehouse Faults on Plate 3. The age of sericitic alteration is younger than potassic alteration because veins with sericite selvages cut and offset biotite veinlets. The age of the sericitic alteration with respect to sodic alteration is unclear, but it is probably younger.

Veins with sericite selvages cut rocks that have undergone sodic alteration.

Assemblages

There are two sericitic alteration assemblages in the Wheeler Mine area: strong and moderate (Table 4). The strong sericitic assemblage is characterized by quartz, sericite, and pyrite replacing almost all other minerals. Only trace amounts of relict igneous plagioclase may remain; most plagioclase has been sericitized and albitized. This alteration has destroyed the texture of the hostrock. In strong sericitic alteration, the rock typically consists of 55-65 volume percent quartz, 35-40 volume percent sericite, and about 5 volume percent of Fe-oxides: jarosite and hematite derived from weathering and oxidation of approximately 5% pyrite. Also trace amounts of rutile maybe present.

The moderate sericitic assemblage is a superposition of the partial sericitic alteration on top of the potassic-sodic 4 assemblage (Table 4, Plates 3). This assemblage is characterized by plagioclase and albite having been partially altered to sericite, typically about 5-10%. Sericite also has replaced up to 5% of the total biotite present. Trace amounts of igneous biotite and hydrothermal biotite are altered to chlorite. Trace amounts of relict

igneous biotite and magnetite remain. The presence of biotite in this assemblage is unusual, and it is probably due to the regional metamorphic event. The sericitic alteration altered the biotite to chlorite + sericite, and the metamorphic event altered the chlorite + sericite back to biotite + sericite (see above). Hematite has replaced the trace amount pyrite that was present.

Veins

Numerous pyrite veins are present in the strong sericitic assemblage. These veins are up to 4 mm wide and have selvages of sericitized and albitized plagioclase. The veins are so numerous and the rock is so strongly altered that the selvages overlap so their outlines are difficult to determine. The pyrite veins have densities up to 15%. The pyrite veins cut, but do not offset quartz-sulfide veins so their age is not assured: the pyrite veins are likely younger, but they could be older if quartz replaced the wallrock next to the pyrite veins.

The moderate sericitic assemblage does not have any veins associated with it.

Metamorphic Alteration

Distribution and Age

The weak biotitization (Table 4, Plates 3 and 4) in the Wheeler Mine area is metamorphic in origin, as discussed below. This metamorphic assemblage is present throughout the approximately 73 km^2 of exposures of the granodiorite of Lobdell Summit (Nowark, 1979; Stewart and others, 1981; John and others, in press). In the northern part of the pluton, magmatic hornblende is uncommon due to replacement by biotite whereas in the southern part of the pluton there is 10-30 volume percent igneous hornblende present with lessor replacement biotite. This pervasive alteration is likely due to a metamorphic event which has also affected other Triassic and early Jurassic plutonic, volcanic, and sedimentary rocks in the region (Dilles and Wright, 1988).

The metamorphic assemblage in the Wheeler Mine area occurs to the west of hornblende granite porphyry and quartz porphyry dikes in the granodiorite of Lobdell Summit and west of the strong hydrothermal alteration assemblages described above (Plates 1 and 3). The only exception to this is the large block of granodiorite of Lobdell Summit in the Wheeler granite porphyry (Plates 1 and 3). This block of granodiorite is interpreted to be faulted into place, but no faults are apparent on the surface.

Assemblage

The metamorphic assemblage is characterized by secondary shreddy biotite that partially, typically 60-70%, replaces magmatic hornblende and some, generally less than 5%, calcic plagioclase that is lightly dusted with biotite. Aligned biotite forms a weak foliation in the rock (Figure 11). Plagioclase grains are zoned and lightly dusted with fine-grained sericite. Very trace amounts of epidote also replace plagioclase grains. Rutile is present in biotite cleavages due to exsolution from biotite during alteration. Relict igneous hornblende, oligoclase, microcline, biotite, magnetite and ilmenite are still present in this assemblage.

Mineralization

Mineralization in the Pine Grove District occurs predominantly between the Wheeler and Stonehouse Faults (Plates 3 and 5). Both the gold and copper sulfide mineralization is associated with the transitional veins.

The total amount of sulfides present in the transitional veins and vein selvages never exceeds more than 1-2 volume percent, and is generally much less. Sulfide mineralization is largely in sulfide veins, with lesser amounts of sulfides occurring as disseminated grains or in quartz-sulfide veins. Relative sulfide volumes are:

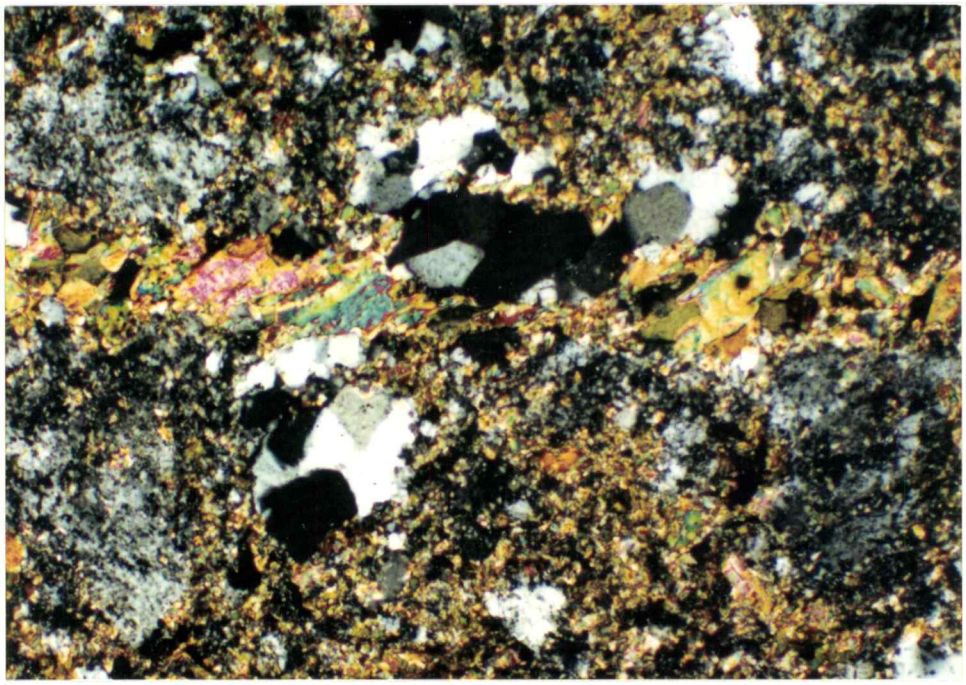

Figure 11. Photomicrograph illustrating a hydrothermal (potassic) biotite vein in which metamorphic recrystallization has aligned biotite into a foliation at 40° to vein strike.

disseminated sulfide > quartz-sulfide veins > Cp-Py veins. Disseminated sulfide minerals consist of pyrite, chalcopyrite, and marcasite (Py>Cp>>Mc), and they commonly occur in aggregates of biotite (and/or chlorite). Disseminated sulfide minerals generally occur around sulfide and quartz-sulfide veins. This is interpreted to indicate that the most of the disseminated sulfide mineralization was introduced at the same time that the Cp-Py and quartz-sulfide veins were formed within the transitional hydrothermal stage.

Marcasite occurs in quartz-sulfide and sulfide veins, or as rare disseminated grains usually in biotite aggregates. The marcasite has a cracked and pitted texture, and grains are typically about 0.4 mm in diameter, but can be up to 2 mm in diameter. Figure 12 is a photomicrograph of marcasite which illustrates its the texture. Marcasite occurs as inclusions in chalcopyrite, pyrite, and magnetite and has inclusions of pyrite. Marcasite is interpreted to be replacing pyrrhotite as described by Davis and others (1987). Very rare grains of pyrrhotite still remain as small (less than 0.1 mm in diameter) inclusions in other sulfide minerals with the exception of marcasite.

The replacement of pyrrhotite by marcasite can be done by sulfidation or iron loss (Schoonen and Barnes, 1991), and sulfidation is the most likely process in the Pine Grove District for the presence of marcasite. Schoonen and Barnes

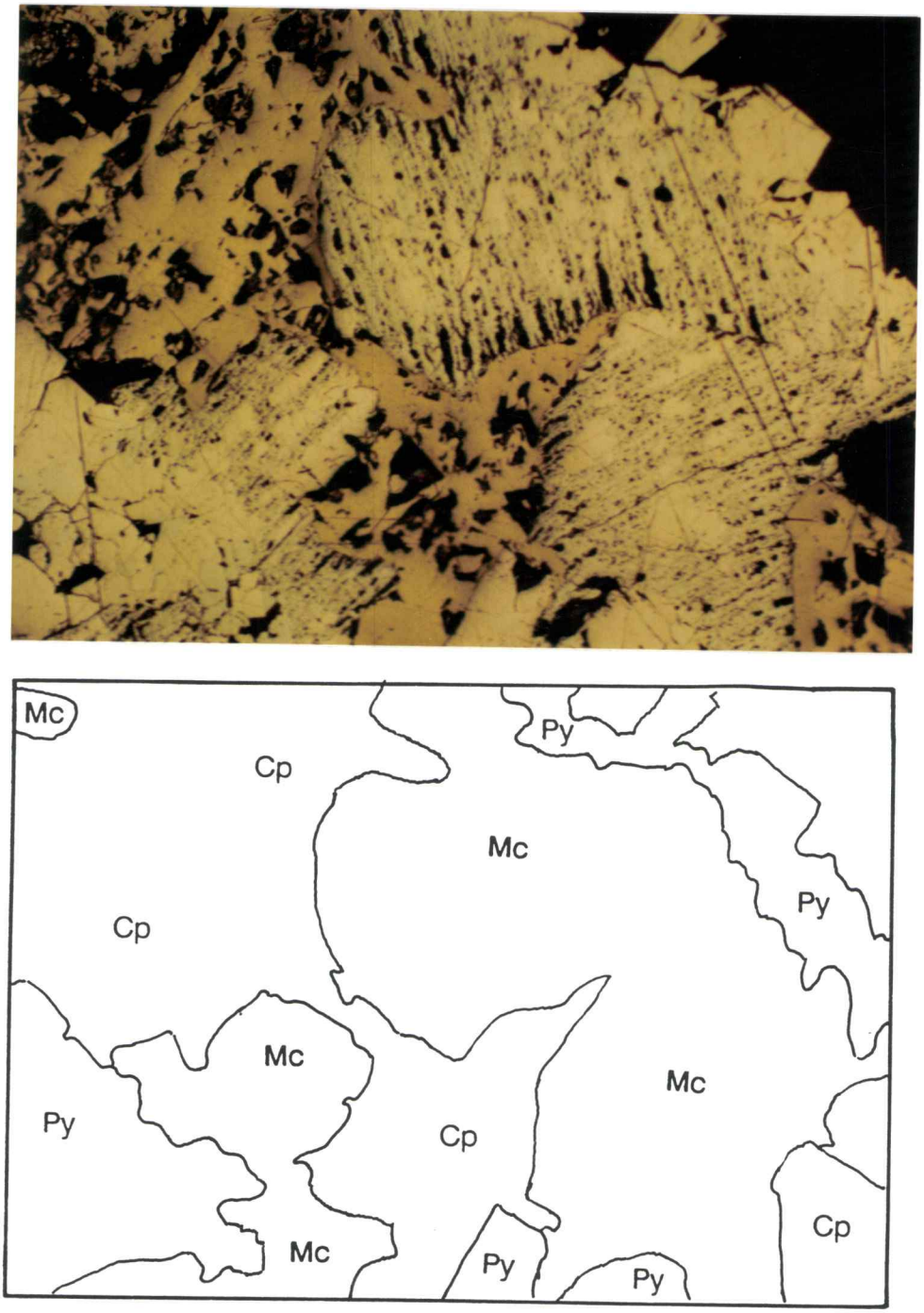

Figure 12. Photomicrograph illustrating the pitted and cracked texture of marcasite.

(1991) experimental work shows that iron loss might be of major importance in the formation of marcasite if no sulfur source were available. These experiments indicate that pyrrhotite alters to marcasite between 100° and 250°C in acidic solutions (Schoonen and Barnes, 1991). In solutions that were neutral or basic, pyrrhotite altered to pyrite. The sulfidation of pyrrhotite to marcasite under acidic conditions probably occurred as a result of the early pyrrhotite and pyrite assemblages of the transitional veins being attacked by lower pH fluids of the younger sericitic alteration at the Pine Grove District.

Copper mineralization at the Wheeler Mine is characterized by chalcopyrite. Weathering within 30 m of the surface has altered trace amounts of chalcopyrite on the surface to glassy limonite, and minor amounts of chrysacolla occur as staining along fractures.

The copper grade can be several thousand ppm over a 5 ft interval, but it is most commonly only several hundred ppm. Plates 3 and 5 illustrate the surface and subsurface copper grade at the Wheeler Mine. Copper sulfide mineralization tends to occur lower in the mine area (Plate 5). The subsurface samples in the Wheeler Mine have higher copper grades than the surface samples. This could be due to supergene weathering which remobilized the copper and partially removed it in the oxidized zone within 30 m of the surface.

Gold has only been identified in the quartz-sulfide veins (Table 5) in the Pine Grove District, as described above. Native gold typically occurs on the margins of pyrite or chalcopyrite grains, but can occur interstitially between quartz grains in the veins or as inclusions in pyrite grains. No native gold was found outside of the veins as disseminated grains with or without sulfide minerals. In the Wheeler Mine area, higher densities of these quartz-sulfide veins correlate with higher gold grades. Figures 13a and 13b are plots of gold grades and visually estimated quartz-sulfide vein densities for the core holes WD-1 and WD-2. Plate 6 has plots of gold grade and quartz-sulfide vein densities. There is a excellent positive correlation between gold grade and quartz-sulfide vein densities in both plots.

There is moderate positive correlation between high gold and copper grades. This is consistent with the observation that all of the gold and the bulk of the copper occur in quartz-sulfide veins, and that Au and Cu are deposited in the same vein/fluid conduits. The richer gold grades tend to occur higher in the mine area whereas richer copper grades tend to occur lower in the mine area. This slight spatial separation of gold and copper centers suggests slightly different controls on mineralization, perhaps due to declining temperature and pressure or changes in chemical composition upward in fluids moving through the veins.

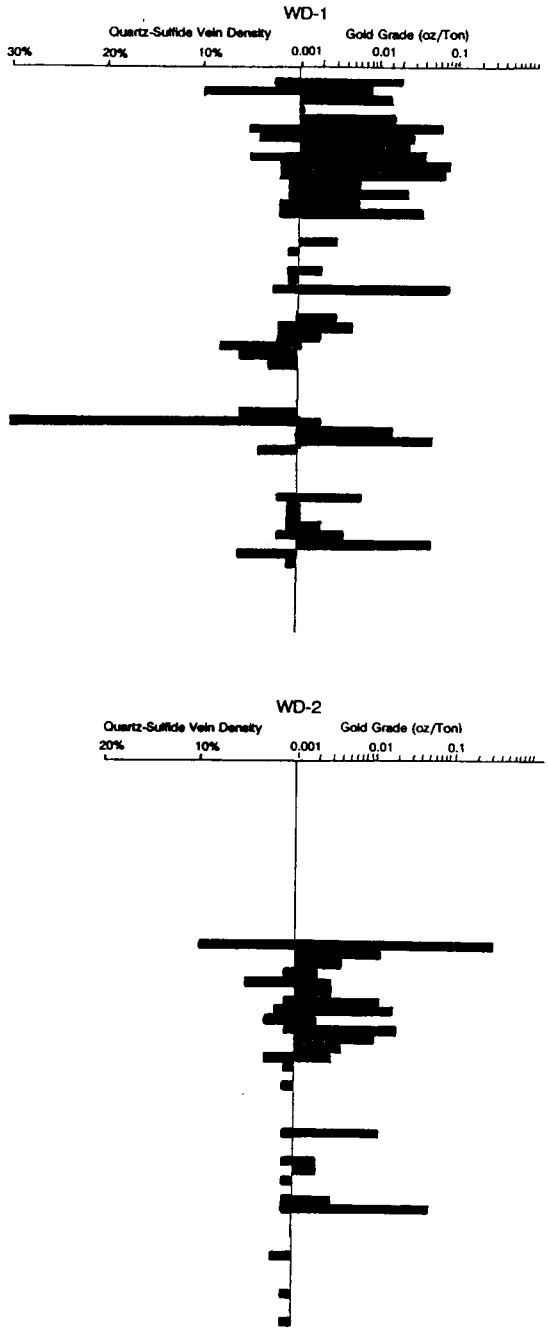

Figure 13. Plots of quartz-sulfide vein densities and gold grades for core drill holes WD-1 and WD-2.

The gold and copper sulfide mineralization occurs in the granodiorite of Lobdell Summit and the microdiorite dikes that have been altered to a potassic-sodic 4 or 5 assemblage and cut by transitional vein assemblages. This mineralization occurs between the Wheeler and Stonehouse Faults, and to a lesser extent, below the Stonehouse Fault in the granodiorite. The gold and copper grades in the granodiorite below the Stonehouse Fault are lower by a factor of 10 than the grades above the fault. The fault has juxtaposed more mineralized rock in the hanging wall from high in the hydrothermal system against less mineralized rock in the footwall from lower in the hydrothermal system.

Faulting occurred after hydrothermal alteration and mineralization in the mine area. The Tertiary faults (described earlier) bound and juxtapose markedly different gold and copper grades in the mine (Plate 5). They also offset quartz-sulfide veins. Faults containing clayey gouge and associated with brittle deformation can contain quartz-sulfide vein fragments and rock flour; the faults containing vein fragments commonly have high gold grade (Plate 6).

The mineralization in the sericitic assemblages is characterized by pyrite as the only or predominant sulfide. I estimated petrographically, from oxidized samples, that there were originally 2-4% pyrite within the strong sericitic assemblage. The ratio of disseminated pyrite to vein pyrite is estimated to be 1:1 to 2:1. The pyrite has

undergone weathering and has been altered to a mixture of hematite and jarosite, which strongly stains the rocks. The weak sericitic assemblage had trace amounts of disseminated pyrite which has weathered to hematite.

In contrast to the transitional assemblages, the sericitic assemblages apparently did not have any gold or copper mineralization associated with them. Surface sampling by Teck Resources Inc. and the author (sample DSP-57, Table 3 and Appendix 4) did not contain any detectable Au and Cu (<1 ppb, < 10 ppm), and there is no indication that there was any originally. This indicates that the strong pervasive sericitic alteration is different event from transitional veins that are characterized by narrow, partially sericitized selvages.

Summary and Conclusions

The Pine Grove district is a gold-rich copper porphyry deposit characterized by rock containing 1-2 ppm Au and 200-300 ppm Cu in quartz-pyrite-chalcopyrite veins. The deposit has hydrothermal alteration assemblages (i.e., potassic, sodic, and sericitic) and sulfide mineralization (i.e. chalcopyrite and pyrite) that are typical of other porphyry type deposits (e.g., Yerington, Nevada; Dilles and Einaudi, 1992). This alteration and mineralization is associated spatially and temporally with granite porphyry dike intrusions. Potassic alteration is characterized by secondary biotite and is comparable to other gold-rich deposits described by Sillitoe (1990).

The gold and copper sulfide mineralization occurred within vein assemblages that were transitional from earlier potassic and sodic alteration to later sericitic alteration. These transitional veins are characterized by quartz + pyrite + chalcopyrite and have narrow selvages containing minor hydrothermal chlorite + sericite + albite, whereas the later pyrite-rich veins of sericitic alteration have wide selvages of pervasive quartz-sericite. The original pyrite + chalcopyrite + pyrrhotite + chlorite mineralogy of the transitional vein sulfide assemblages indicates a low sulfur fugacity and relatively reduced conditions at the time of mineralization (e.g., Beane and Titley, 1981). The

pyrite-rich sulfide assemblage (Py ± Cp ± Mc) of the sericitic alteration indicates a higher sulfur fugacity, and less reduced condition of formation than those of the transitional veins.

The geology of the Pine Grove District is complex due to a series of events beginning with pluton emplacement and associated hydrothermal alteration, followed by metamorphic alteration, and ending with Tertiary deformation. A summary of these events is presented in Figure 14.

The granodiorite of Lobdell Summit in the Pine Grove District was emplaced in the late Triassic or early Jurassic. It has two whole-rock Rb-Sr ages of 186.9±8.5 Ma (John and others, 1991) and 186.5±7.7 Ma (Robinson and Kistler, 1986). The whole-rock Rb-Sr ages could be the emplacement age of the granodiorite or they could be the age of a early to middle Jurassic regional metamorphic event, which is documented at this time in the Yerington District (Dilles and Wright, 1988).

Shortly after the emplacement of the granodiorite, a series of granitic dikes intruded the Pine Grove District. These dikes are genetically related to the granodiorite because they have similar major and trace element patterns (Figure 5), and hence were likely emplaced within less than a million years after the granodiorite. These dikes are also spatially and temporally related to hydrothermal alteration

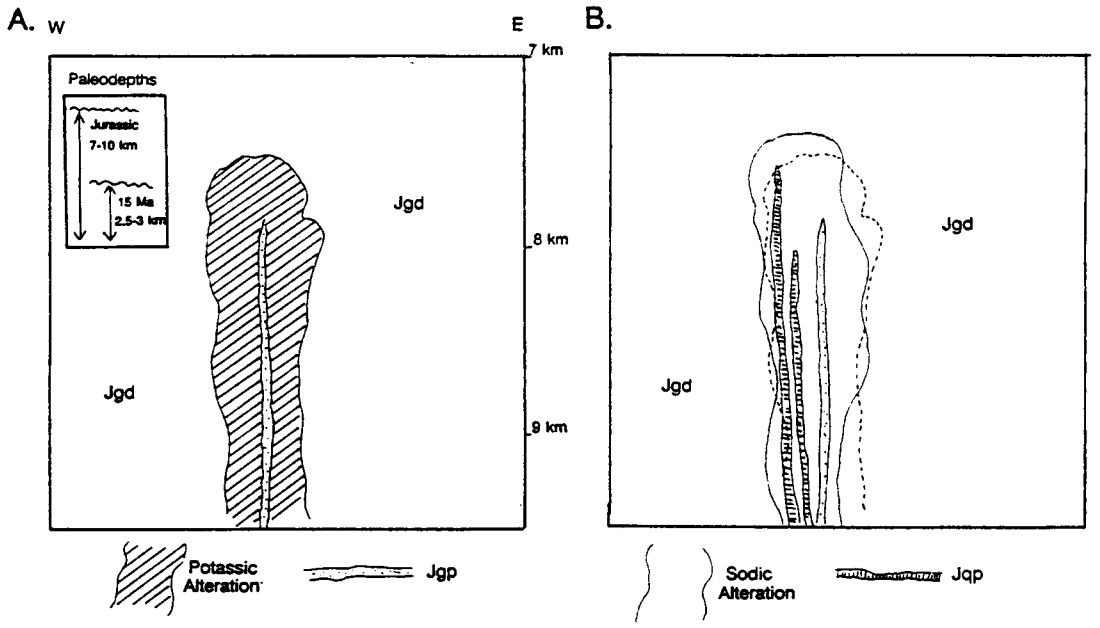

Figure 14. Diagram summarizing the geologic history of the Wheeler Mine as a cross section looking north 30° west.

A. Emplacement of the Wheeler granite porphyry dike and potassic hydrothermal alteration during the Early (?) Jurassic.

B. Emplacement of the quartz porphyry and hornblende granite porphyry dikes, and sodic hydrothermal alteration during the Early (?) Jurassic.

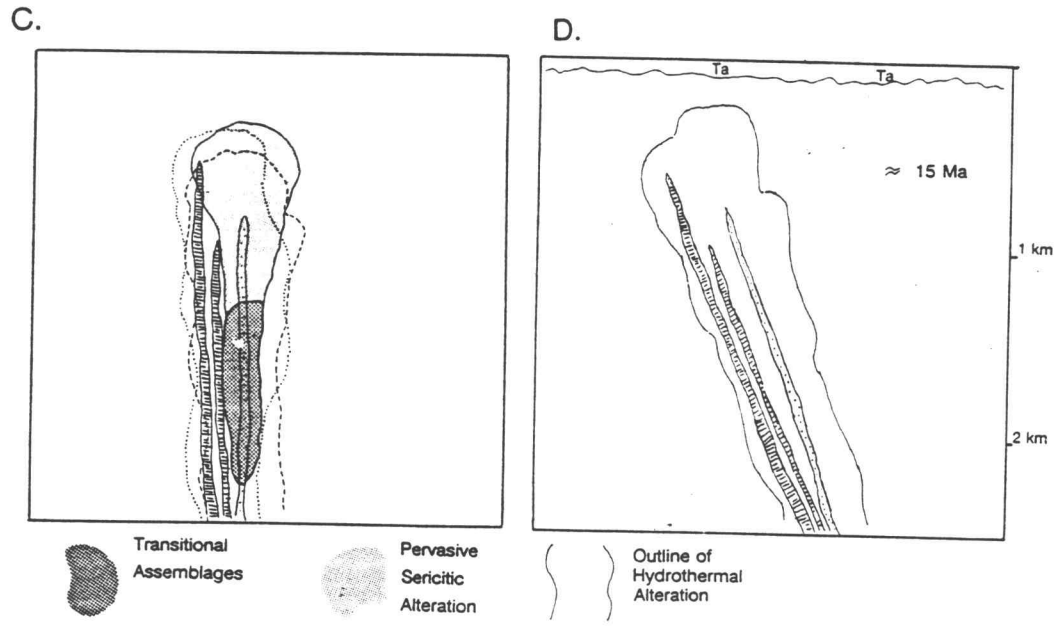

Figure 14 continued.

C. Transitional quartz-sulfide and sulfide (Cp-Py) veins and Au-Cu mineralization, followed by pyrite veins and sericitic alteration during the Early (?) Jurassic.

D. Metamorphic deformation (Early or Middle Jurrassic); ≈3-6 km of uplift and erosion; 20-25° westward tilting between Early (?) Jurassic and 15 Ma; eruption of 17-14 Ma volcanic rocks (Ta).

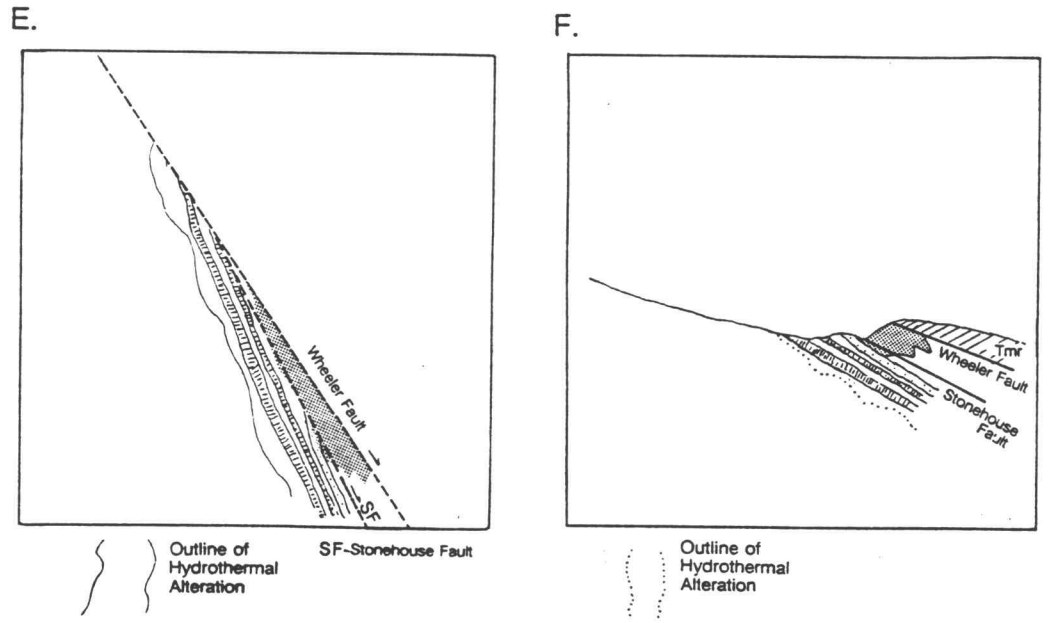

Figure 14 continued.

E. The location of Cenozoic Basin and Range faults, schematically showing offset on the Stonehouse Fault prior to tilting.

F. Present day cross section after tilting associated with movement on the Wheeler and Stonehouse Faults and after erosion.

and mineralization. The hydrothermal events are centered around the dikes, and the dikes were emplaced while the hydrothermal activity took place. These field and age relations establish that the hydrothermal events are bracketed by emplacement of early and late dikes.

In the Pine Grove District, the granodiorite of Lobdell Summit was emplaced at 7-10 km paleodepth based on hornblende geobarometry. Due to the granitic dikes having a similar magmatic source as the granodiorite, they are also assumed to be emplaced at the same depth. Paleo-stratigraphic estimates based on cross-sections indicate that the Pine Grove District was at least 3-4 km paleodepth during mineralization.

The Wheeler granite porphyry was the first intrusive event, and it was followed by volumetrically smaller dikes of microdiorite and monzonite. After these dikes were emplaced, potassic alteration characterized by shreddy biotite replacing hornblende and locally plagioclase took place. Figure 14a illustrates the emplacement of the Wheeler granite porphyry dike and potassic alteration.

The quartz porphyry and hornblende granite porphyry dikes were intruded next. Hornblende was not replaced by hydrothermal biotite in these dikes, and hence the hornblende granite porphyry is interpreted to post-date potassic alteration. After these dikes were emplaced, sodic alteration took place. This event was characterized by

albite replacing potassium feldspar, and oligoclase and albite replacing magmatic plagioclase. Locally, actinolite and chlorite replace hornblende and biotite. Figure 14b illustrates the emplacement of the quartz porphyry and hornblende granite porphyry dikes and sodic alteration. In the Wheeler Mine area, sodic assemblages are widely superimposed on potassic assemblages as evidenced by actinolite veins cross cutting biotite veinlets. The resulting assemblages contain both potassic and sodic index minerals and have been mapped as mixed, potassic-sodic assemblages.

The transitional veins and vein selvages were formed next (Figure 14c). Quartz + pyrite + chalcopyrite + marcasite ± magnetite ± pyrrhotite veins containing gold were formed early and were followed by chalcopyrite + pyrite ± quartz ± marcasite veins. Disseminated sulfide mineralization was characterized by pyrite, chalcopyrite, and pyrrhotite, and it was localized around the sulfide veins and to a lesser extent, around the quartz-sulfide veins.

The last hydrothermal event was sericitic alteration that accompanied pyrite veins. The sericitic alteration is characterized by zones in which all minerals are replaced by sericite, quartz, and 5% disseminated pyrite. The sericitic alteration locally affected all of the Mesozoic granitic dikes in the district. Since albite is much more stable than

plagioclase in sericitic alteration, rocks that had previously undergone strong sodic alteration were not as effected by sericitic alteration as other rocks. Figure 14c outlines sericitic alteration and transitional assemblages.

The next major event in the Pine Grove District was a regional greenschist metamorphic event characterized by growth of metamorphic biotite, development of a weak foliation in mica, and minor ductile deformation. Dilles and Wright (1988) constrained the age of this event as pre-169 Ma and post early Jurassic, and also post-dating the 233 Ma Wassuk Diorite (that is Middle to Late Triassic) pluton in the Yerington District. This event affected other Triassic and early Jurassic plutonic, volcanic, and sedimentary rocks in the region. This event probably altered chlorite + phengitic sericite to biotite in zones of partial sericitic alteration at the Wheeler Mine.

The granitic dikes were probably tilted 20-25° westerly to dips of 65-70° east during the metamorphic deformation or during a later deformation prior to 15 Ma. Figure 14d illustrates the tilting of the granitic dikes prior to 15 Ma. There was a period of erosion in the region following metamorphism and prior to 15 Ma that may have removed 3-6 km of material in the area of the district. This was followed by volcanism at 17-14 Ma that erupted up to 1-2 km of andesite and dacite flows and breccias.

Tertiary deformation in the district between 15-7.5 Ma is characterized by normal faults and brittle, cataclastic deformation. This deformation tilted the granitic dikes approximately 30-40° to the west to their present dip of 30-35° to the east. The westerly tilting is associated with movement on the Wheeler Fault and other faults of the Pine Grove Hills fault system. One strand, the Stonehouse fault also moved a block of granodiorite that had sericitic alteration and transitional veins containing gold mineralization down approximately 1 km next to rocks that were deeper in the system. Figure 14e is a diagram of the district before the tilting from the Tertiary deformation but after Tertiary faulting. Figure 14f is how the district appears presently after Cenozoic tilting and erosion.

BIBLIOGRAPHY

Anders, E., and Ebihara, M., 1982, Solar-system abundances of the elements: Geochim. et Cosmochim. Acta., v. 46, p. 2363-2380.

Axelrod, D.I., 1956, Mio-Pliocene floras from west-centrl Nevada: California Univ. Pubs. Geol. Sci., v. 33, p. 1-322.

Beane, R.E., and Titley, S.R., 1981, Porphyry copper deposits, Part II: Hydrothermal alteration and mineralization: Econ. Geol. 75TH Anniv. Vol., p. 235-269.

Burnham, C.W., 1979, Magmas and hydrothermal fluids, in Barnes, H.L., ed., Geochemistry of hydrothermal ore deposits, 2nd Ed.: New York, Wiley Intersci., p. 71-136.

Carten, R.B., 1986, Sodium-calcium metasomatism: chemical, temporal, and spatial relationships at the Yerington, Nevada, porphyry copper deposit: Econ. Geol., v. 73, p. 1270-1286.

Couch, C.V. and Carpenter, J.A., 1943, Nevada's metal and mineral production (1859-1940): University of Nevada Bull. no. 38, 159p.

Davis, E.E., Goodfellow, W.D., Bornhold, B.D., Adshead, J., Blaise, B., Villinger, H., and Le Cheminant, G.M., 1987, Massive sulfides in a sedimented rift valley, northern Juan de Fuca Ridge: Earth Planet. Sci. Letters, v. 82, p. 49-61.

Dilles, J.H., 1984, The petrology and geochemistry of the Yerington batholith and the Ann-Mason porphyry copper deposit, western Nevada: Unpub. Ph.D. thesis, Sanford Univ., 389 p.

Dilles, J.H., 1987, Petrology of the Yerington Batholith, Nevada: evidence for evolution of porphyry copper ore fluids: Econ. Geol., v. 82, p. 1750-1789.

Dilles, J.H., and Einaudi, M.T., 1992, Wall-rock alteration and hydrothermal flow paths about the Ann-Mason porphyry copper deposit, Nevada: Econ. Geol., v. 87, p. 1963-2001.

Dilles, J.H., and Wright, J.E., 1988, The chronology of early Mesozoic arc magmatism in the Yerington district of western Nevada and its regional implications: Geol. Soc. America Bull., v. 100, p. 644-652.

Dircksen, P.E., 1975, Geology and mineralization of the Pine Grove-Rockland Mining Districts, Lyon County Nevada: Unpub. M.S. thesis, University of Nevada-Reno, 60p.

Flanagan, F.J., 1976, 1972 compilation of data on USGS standards: U.S. Geol. Survey Prof. Paper 840, p. 131-183.

Gilbert, C.M., and Reynolds, M.W., 1973, Character and chronology of basin development, western margin of the Basin and Range Province: Geol. Soc. America Bull., v. 84, p. 2489-2510.

Gilluly, J., 1933, Replacement origin of the albite granite near Sparta, Oregon: U.S. Geol. Survey Prof. Paper 175-C, p.65-81.

Gromet, L.P., and Silver, L.T., 1983, Rare earth element distributions among minerals in a granodiorite and their petrogenetic implications: Geochim. et Cosmochim. Acta., v. 47, p. 925-939.

Hammarstrom, J.M., and Zen, E., 1986, Aluminum in hornblende: an empirical igneous geobarometer: Am. Mineralogist, v. 71, p. 1297-1313.

Hill, J.M., 1915, Some mining districts in northeastern California and northwestern Nevada: U.S. Geol. Survey Bull. 594, p. 133-141.

Hollister, L.S., Grisson, G.C., Peters, E.K., Stowell, H.H., and Sisson, V.B., 1987, Confirmation of the empirical correlation of Al in hornblende with pressure of solidification of calc-alkaline plutons: Am. Mineralogist, v. 72, p. 231-239.

John, D.A., Schweickert, R.A., and Robinson, A.C., in press, Granitic rocks in the Reno centerpiece study area: U.S. Geol. Survey Bull.

Johnson, M.C., and Rutherford, M.J., 1989, Experimental calibration of the aluminum-in-hornblende geobarometer with application to Long Valley caldera (California) volcanic rocks: Geology, v. 17, p. 837-841.

Krueger, H.W., and Schilling, J.H., 1971, Geochron/Nevada Bureau of Mines K/Ar age determinations, list 1: Isochron/West, no. 71-1, p. 9-15.

Lanier, G., Raab, W.J., Folson, R.B., and Cone, S., 1978, Alteration of equigranular monzonite, Bingham Mining District, Utah: Econ. Geol., v. 73, p. 1270-1286.

Lincoln, F.G., 1923, Mining districts and mineral resources of Nevada: Reno, Nevada Newsletter Publishing Co., p. 148-149.

Meyer, C., and Hemley, J., 1967, Wall rock alteration, in Barnes, H., ed., Geochemistry of hydrothermal ore deposits: Holt, Rinehart, and Wilson, Inc., New York, p. 166-235.

Miyashiro, A., 1973, Metamorphism and metamorphic belts, 1st ed.: London, William Crowes and Sons Ltd., 492 p.

Moore, J.G., and Archbold, N.L., 1969, Geology and mineral deposits of Lyon, Douglas, and Ormsby Counties, Nevada: Nevada Bur. Mines and Geol. Bull. 75, 45p.

Nowak, G., 1979, The geology and uranium occurences of the Washington Mining District, Lyon County, Nevada: Unpub. M.S. thesis, University of Nevada-Reno, 92p.

Robinson, A.C., and Kistler, R.W., 1986, Maps showing isotopic dating in the Walker Lake 1° by 2° quadrangle, California and Nevada: U.S. Geol. Survey Misc. Field Studies Map MF-1382-N, scale 1:250,000.

Schoonen, M.A.A., and Barnes, H.L., 1991, Mechanisms of pyrite and marcasite formation from solution: III. hydrothermal processes: Geochim. et Cosmochim. Acta., v. 55, p. 3491-3504.

Steiger, R.H., and Jager, E., 1977, Subcommission on geochronology: convention on the use of decay constants in geo- and cosmochronology: Earth Planet. Sci. Letters, v. 36, p. 359-362.

Stewart, J.H., and Reynolds, M.W., 1987, Geologic map of the Pine Grove Hills quadrangle, Lyon County Nevada: U.S. Geol. Survey Open-File Report 87-658, scale 1:62,000, 8p.

Stewart,J.H., Reynolds, M.W., and Johanesen, D.C., 1981, Geologic map of the Mount Grant quadrangle, Lyon and Mineral Counties, Nevada: U.S. Geol. Survey Misc. Field Studies Map MF-1278, scale 1:62,500.

Stoddard, C., and Carpenter, J.A., 1950, Mineral resources of Storey and Lyon Counties, Nevada: University of Nevada Bull. no. 49, p. 95-98.

Streckeisen, A., 1976, To each plutonic rock its proper name: Earth-Sci. Rev., v. 12, p. 1-33.

Suzuki, K., Adachi, M., and Yamamoto, K., 1990, Possible effects of grain-boundary REE on the REE distribution in felsic melts derived by partial melting: Geochem. Jour.,v. 24, p. 57-74.

Swanson, S.E., and Fenn, P.M., 1986, Quartz crystallization in igneous rocks: Am. Mineralogist, v. 71, p. 331-342.

APPENDICES

Appendix 1

Electron Microprobe Analyses of Titanite

Rock Type	Granodiorite of Lobdell Summit				Wheeler Granite Porphyry			
Sample Number	DSP 201				DSP 16			
Location	core	core	core	rim	core	core	core	rim
Wt. %								
SiO_2	30.66	29.92	29.46	28.71	28.99	29.10	28.88	30.92
TiO_2	38.85	38.15	36.70	36.64	35.83	35.93	36.38	36.34
Al_2O_3	0.86	1.13	1.51	1.42	1.17	1.27	1.22	1.80
Y_2O_3	0.05	0.09	0.88	0.69	0.53	0.44	0.44	0.25
Ce_2O_3	0.00	0.00	0.00	0.02	1.03	1.11	0.97	0.04
Nd_2O_3	0.00	0.00	0.01	0.07	0.67	0.73	0.68	0.05
Sm_2O_3	0.00	0.01	0.01	0.06	0.16	0.17	0.16	0.02
Gd_2O_3	0.01	0.03	0.08	0.12	0.28	0.21	0.19	0.03
Dy_2O_3	0.04	0.03	0.14	0.11	0.06	0.06	0.10	0.02
Yb_2O_3	0.00	0.03	0.12	0.04	0.04	0.05	0.00	0.01
MgO	0.03	0.00	0.00	0.00	0.02	0.04	0.02	0.02
CaO	28.26	28.05	26.91	27.35	26.12	26.37	26.47	27.75
MnO	0.10	0.10	0.00	0.02	0.11	0.10	0.08	0.00
FeO	0.67	0.79	1.06	0.83	1.66	1.72	1.60	1.00
H_2O*	3.79	0.75	1.64	5.26	2.42	1.01	2.63	1.07
F	0.13	0.20	0.15	0.01	0.02	0.03	0.05	0.17
Cl	0.01	0.01	0.17	0.01	0.00	0.01	0.00	0.00
Total	103.46	99.20	98.93	101.36	99.11	98.25	99.87	99.58

* calculated by Stoichiometry assuming the Σ cations equals 20 with 4 cations of Si.

Appendix 2

Electron Microprobe Analyses of Allanite

Rock Type	Granodiorite of Lobdell Summit							
Sample Number	DSP 39B		DSP 48		DSP 59		DSP 151	
Location	core	rim	core	rim	core	rim	core	rim
Wt.%								
MgO	1.21	0.05	1.11	1.27	1.06	0.81	1.24	1.28
Al_2O_3	12.83	22.57	13.14	12.44	12.96	14.62	11.89	11.58
SiO_2	29.79	36.09	29.70	30.27	30.29	30.64	29.22	28.85
CaO	10.11	19.52	9.53	9.48	9.82	10.67	9.81	9.89
TiO_2	1.57	0.14	1.48	1.67	1.25	0.85	2.08	2.17
MnO	0.53	0.42	0.66	0.45	0.53	0.66	0.54	0.52
Fe_2O_3	17.32	12.73	17.20	17.42	17.34	16.23	17.85	18.03
Y_2O_3	0.12	0.18	0.17	0.11	0.06	0.11	0.17	0.09
La_2O_3	8.63	1.60	9.64	9.85	8.87	8.16	9.45	9.96
Ce_2O_3	13.28	2.60	13.01	12.97	13.15	12.58	13.30	12.95
Nd_2O_3	1.78	0.28	1.49	1.53	1.69	1.74	1.53	1.46
Sm_2O_3	0.25	0.02	0.16	0.19	0.22	0.24	0.22	0.18
Gd_2O_3	1.31	0.30	1.38	1.34	1.22	1.30	1.29	1.33
Dy_2O_3	0.00	0.00	0.00	0.00	0.00	0.00	0.00	0.00
Yb_2O_3	0.02	0.02	0.05	0.00	0.00	0.00	0.00	0.05
ThO_2	0.20	0.08	0.44	0.69	0.90	1.02	0.35	0.35
UO_2	0.00	0.00	0.02	0.00	0.00	0.00	0.00	0.02
Total	98.95	96.60	99.18	99.72	99.36	99.63	98.94	98.71

Appendix 3

Electron Microprobe Analyses of Ilmenite and Magnetite

Rock Type	Granodiorite of Lobdell Summit							
Sample Number	DSP 201				DSP 201			
Mineral	mag	mag	mag	mag	ilm	ilm	ilm	ilm
Wt. %								
V_2O_5	0.20	0.23	0.24	0.22	0.36	0.32	0.39	0.38
SiO_2	0.00	0.02	0.03	0.00	0.00	0.02	0.02	0.00
TiO_2	0.07	0.03	0.04	0.04	51.23	50.63	51.61	50.33
Al_2O_3	0.04	0.06	0.06	0.04	---	---	---	---
Cr_2O_3	0.01	0.00	0.00	0.01	---	---	---	---
Fe_2O_3	68.03	68.08	67.90	67.92	2.44	3.38	1.88	4.14
MgO	0.00	0.01	0.00	0.01	0.15	0.16	0.14	0.12
MnO	0.08	0.11	0.12	0.11	7.92	6.75	8.43	7.62
FeO	30.69	30.60	30.54	30.54	37.77	38.41	37.62	37.33
ZrO	---	---	---	---	0.08	0.08	0.02	0.03
NbO	---	---	---	---	0.10	0.06	0.11	0.05
Total	99.12	99.14	98.93	98.89	100.05	99.81	100.22	100.00
X_{usp}	0.002	0.001	0.001	0.001	---	---	---	---
X_{ilm}	---	---	---	---	0.974	0.965	0.980	0.957

X_{usp} and X_{ilm} were calculated by method of Stormer (1983).

Appendix 4. Trace Element Compositions of the Mesozoic Rocks in the Pine Grove District, Lyon County Nevada.

Rock Type	Granodiorite of Lobdell Summit				
Sample Number	DSP 6	DSP 8	DSP 39	DSP 55	DSP 57
(ppm)					
Sc	14.3	14.1	17.5	17.2	12.2
V	88	144	117	99	80
Cr	14	13	25	18	12
Co	10.9	9.8	10.9	7.4	0.29
Ni	6	8	10	8	3
Cu	12	41	42	6	0
Zn	46	18	41	14	4
Ga	15	16	14	16	14
Pb	13	0	3	3	1
As	2.9	2.1	12.8	11.0	5.4
Sb	0.5	0.3	0.7	0.4	0.4
Se	0.5	2.4	2.9	2.6	2.0
Rb	98	87	19	85	70
Cs	3.6	1.7	0.34	2.7	1.0
Sr	254	31	237	137	19
Ba	1270	675	111	627	620
La	19.4	3.8	15.3	19.5	8.5
Ce	40.2	10.2	32.6	38.9	16.8
Nd	18.6	4.0	14.2	21.8	4.2
Sm	3.41	1.51	3.31	4.19	1.60
Eu	0.88	0.18	0.90	0.88	0.19
Tb	0.53	0.18	0.50	0.48	0.22
Yb	2.42	1.52	2.16	1.78	1.51
Lu	0.38	1.55	2.25	1.86	1.62
Y	22	10	21	17	15
Zr	153	107	109	122	109
Nb	8.4	4.2	5.4	5.2	6.0
Hf	4.8	3.4	3.2	3.5	3.5
Ta	0.40	0.29	0.29	0.41	0.30
W	3	N.D.	N.D.	N.D.	N.D.
Au	0.02	N.D.	N.D.	N.D.	N.D.
Hg	0.01	N.D.	N.D.	N.D.	N.D.
Th	11.0	7.9	6.0	7.8	5.9
U	2.9	2.9	2.2	2.8	2.9

Appendix 4. continued

Rock Type	Granodiorite of Lobdell Summit			Wheeler Granite Porphyry	
Sample Number	DSP 60A	DSP 60AS	DSP 111	DSP 16	DSP 53
(ppm)					
Sc	16.4	17.5	12.7	6.5	6.7
V	97	115	71	54	44
Cr	17	18	10	12	13
Co	8.9	6.9	7.5	8.4	7.7
Ni	6	5	6	10	10
Cu	151	208	8	0	8
Zn	52	58	35	14	17
Ga	16	21	16	13	16
Pb	11	11	4	4	7
As	4.8	5.5	15	N.D.	N.D.
Sb	0.6	0.4	0.4	0.9	0.6
Se	2.1	3.6	2.1	0.5	0.9
Rb	65	75	66	130	160
Cs	1.3	1.2	2.1	1.0	2.0
Sr	160	99	177	333	430
Ba	428	700	891	1689	1522
La	14.4	17.1	19.6	23.8	21.7
Ce	26.9	28.8	36.2	46.0	42.3
Nd	12.8	13.0	16.0	16.2	13.3
Sm	3.30	3.14	3.75	3.30	4.52
Eu	0.75	0.62	0.80	0.67	0.65
Tb	0.50	0.43	0.47	0.40	0.31
Yb	2.32	2.23	2.50	2.09	1.63
Lu	0.38	0.37	2.82	0.22	1.97
Y	21	18	20	16	15
Zr	141	167	132	150	157
Nb	7.0	6.8	6.0	7.6	6.4
Hf	4.2	5.1	4.1	4.6	4.7
Ta	0.40	0.40	0.36	0.63	0.65
W	N.D.	N.D.	N.D.	2	N.D.
Au	N.D.	N.D.	N.D.	N.D.	N.D.
Hg	N.D.	N.D.	N.D.	N.D.	N.D.
Th	7.9	10.1	10.7	22.7	23.2
U	2.9	4.6	3.1	8.9	8.7

Appendix 4. continued

Rock Type	Micro-diorite	Monzonite	Quartz Porphyry	Hornblende Granite Porphyry
Sample Number	DSP 3	DSP 41	DSP 2	DSP 165
(ppm)				
Sc	8.9	5.4	2.1	9.5
V	113	26	18	90
Cr	4	9	3	4
Co	9.8	4.3	1.2	6.8
Ni	1	11	8	9
Cu	21	2	2	2
Zn	20	10	4	8
Ga	21	13	13	19
Pb	0	0	0	1
As	8.9	4.3	2.1	N.D.
Sb	0.4	0.4	0.2	0.2
Se	1.1	2.0	N.D.	N.D.
Rb	76	95	10	4
Cs	1.8	0.98	0.3	0.21
Sr	130	237	53	109
Ba	816	990	17	6
La	22.9	46.6	25.6	24.2
Ce	47.4	91.4	45.7	45.2
Nd	24.1	32.9	13.9	18.5
Sm	4.48	7.13	2.73	4.15
Eu	1.36	0.63	0.32	0.98
Tb	0.53	0.73	0.32	0.43
Yb	1.86	5.36	1.31	1.81
Lu	1.85	5.86	0.22	2.16
Y	18	35	10	16
Zr	111	187	107	119
Nb	6.6	11.0	8.2	7.0
Hf	3.3	8.1	3.7	3.5
Ta	0.46	1.4	0.7	0.48
W	N.D.	N.D.	N.D.	N.D.
Au	N.D.	0.03	N.D.	N.D.
Hg	N.D.	N.D.	N.D.	N.D.
Th	5.7	48.9	23.2	9.7
U	2.0	12.0	3.9	3.2

Appendix 5

Electron Microprobe Analyses of Biotite

Rock Type	Granodiorite of Lobdell Summit							
Sample Number	DSP 201	DSP 201	DSP 201	DSP 201	DSP 201	DSP 164B	DSP 36	DSP 36
	Ign Bio	Ign Bio	Ign Bio	Ign Bio	Sec Bio	Sec Bio	Sec Bio	Sec Bio
Wt.%								
SiO_2	35.11	35.88	35.25	35.58	36.45	35.41	35.68	34.96
TiO_2	3.99	1.83	1.62	1.70	1.30	2.06	1.85	1.81
Al_2O_3	14.55	15.61	15.75	15.85	16.04	16.68	17.05	16.58
Fe_2O_3	20.63	21.94	21.48	22.23	20.69	22.57	20.29	22.01
MgO	10.08	10.21	10.86	10.51	11.77	9.74	11.05	10.18
CaO	2.10	0.05	0.03	0.02	0.10	0.00	0.04	0.02
MnO	0.48	0.53	0.60	0.53	0.52	0.78	0.46	0.45
Na_2O	0.04	0.02	0.06	0.05	0.03	0.07	0.08	0.10
K_2O	8.53	9.11	9.49	9.69	9.10	9.82	9.90	9.61
H_2O*	3.77	3.90	3.94	4.01	3.85	3.97	3.86	3.88
F	0.55	0.27	0.15	0.09	0.50	0.26	0.48	0.32
Cl	0.07	0.06	0.05	0.07	0.05	0.04	0.06	0.06
Total	99.90	99.41	99.28	100.33	100.40	101.40	100.80	99.98

* calculated by stoichiometry assuming the Σ cations equals 24 with $4(OH)^-$ replacing O^{2-}.

Appendix 5 continued.

Rock Type	Wheeler Granite Porphyry						Quartz Porphyry	
Sample Number	DSP 16	DSP 16	DSP 16	DSP 16	DSP 16	DSP 16	DSP 2	DSP 2
	Ign Bio	Ign Bio	Ign Bio	Sec Bio	Sec Bio	Sec Bio	Ign Bio	Ign Bio
Wt.%								
SiO_2	36.21	35.32	36.01	37.16	35.67	35.83	37.80	37.05
TiO_2	1.70	5.33	1.72	2.05	1.63	1.64	1.85	1.71
Al_2O_3	15.99	15.37	16.26	15.84	16.07	16.51	16.03	15.49
Fe_2O_3	20.55	19.84	20.22	20.00	20.57	21.06	17.73	17.88
MgO	11.42	11.36	11.70	11.36	11.70	11.24	12.16	13.67
CaO	0.00	0.11	0.00	0.00	0.00	0.02	0.02	0.01
MnO	0.18	0.17	0.14	0.18	0.16	0.20	0.08	0.14
Na_2O	0.06	0.04	0.10	0.05	0.09	0.11	0.05	0.06
K_2O	9.91	8.92	9.75	10.13	10.08	9.89	9.68	9.76
H_2O	3.88	3.84	3.84	3.91	3.81	3.94	3.91	3.87
F	0.35	0.51	0.45	0.41	0.47	0.24	0.41	0.46
Cl	0.17	0.12	0.15	0.12	0.15	0.16	0.05	0.11
Total	100.42	100.93	100.34	101.21	100.40	100.84	99.77	100.21

* calculated by stoichiometry assuming the Σ cations equals 24 with $4(OH)^-$ replacing O^{2-}.

Appendix 6. List of Abbreviations.

Act - Actinolite
Alb - Albite
Al_t - Total aluminum
And - Andesine
Bio - biotite
Chl - Chlorite
Cp - Chalcopyrite
Ep - Epidote
Hbl - Hornblende
Hyd - Hydrothermal
Ign - Igneous
Ilm - Ilmenite
Ja - Aplite
Jgd - Granodiorite of Lobdell Summit
Jgp - Wheeler Granite Porphyry
Jhp - Hornblende Granite Porphyry
Jm - Monzonite
Jmd - Microdiorite
Jqp - Quartz Porphyry
Knc - Granite of Nye Canyon
Ksp - Potassium Feldspar
Mag - Magnetite
Mc - Marcasite
Olg - Oligoclase
Part - partial
Po - Pyrrhotite
Py - Pyrite
Qal - Alluvium
Qdr - Tailings and road fill
Qtz - Quartz
Rut - Rutile
Ser - Sericite
St - Strong
Ta - Andesite and dacite flows and breccias
Tcv - Coal Valley Formation
Ti - Titanite
Tr - Rhyolite
Tw - Morgan Ranch Formation
Wt - Weight